

<b>REPORT DOCUMENTATION PAGE</b>			Form Approved OMB NO. 0704-0188		
<p>The public reporting burden for this collection of information is estimated to average 1 hour per response, including the time for reviewing instructions, searching existing data sources, gathering and maintaining the data needed, and completing and reviewing the collection of information. Send comments regarding this burden estimate or any other aspect of this collection of information, including suggestions for reducing this burden, to Washington Headquarters Services, Directorate for Information Operations and Reports, 1215 Jefferson Davis Highway, Suite 1204, Arlington VA, 22202-4302. Respondents should be aware that notwithstanding any other provision of law, no person shall be subject to any penalty for failing to comply with a collection of information if it does not display a currently valid OMB control number.</p> <p>PLEASE DO NOT RETURN YOUR FORM TO THE ABOVE ADDRESS.</p>					
1. REPORT DATE (DD-MM-YYYY) 24-07-2015		2. REPORT TYPE MS Thesis		3. DATES COVERED (From - To) -	
4. TITLE AND SUBTITLE Partial Ordering and Stochastic Resonance in Discrete Memoryless Channels			5a. CONTRACT NUMBER W911NF-11-1-0144		
			5b. GRANT NUMBER		
			5c. PROGRAM ELEMENT NUMBER 206022		
6. AUTHORS Roland-Yannick Kamdem Kenmogne			5d. PROJECT NUMBER		
			5e. TASK NUMBER		
			5f. WORK UNIT NUMBER		
7. PERFORMING ORGANIZATION NAMES AND ADDRESSES The University of the District of Columbia Computer Science and Informati Briana Lowe Wellman Washington, DC 20008 -1122				8. PERFORMING ORGANIZATION REPORT NUMBER	
9. SPONSORING/MONITORING AGENCY NAME(S) AND ADDRESS (ES) U.S. Army Research Office P.O. Box 12211 Research Triangle Park, NC 27709-2211				10. SPONSOR/MONITOR'S ACRONYM(S) ARO	
				11. SPONSOR/MONITOR'S REPORT NUMBER(S) 58962-NS-REP.23	
12. DISTRIBUTION AVAILABILITY STATEMENT Approved for public release; distribution is unlimited.					
13. SUPPLEMENTARY NOTES The views, opinions and/or findings contained in this report are those of the author(s) and should not contrued as an official Department of the Army position, policy or decision, unless so designated by other documentation.					
14. ABSTRACT In this thesis, we study the performance of Discrete Memoryless Channels (DMCs) arising in the context of cooperative underwater wireless sensor networks. We introduce a partial ordering for the binary-input ternary output (2,3) DMC. In the particular case of the Binary Symmetric Channel with Symmetric Erasure (BSC/SE), we use majorization theory, channel convexity and directional derivative in order to obtain a partial solution to the open problem of partial ordering of the DMCs. In addition, we analyze the stochastic resonance					
15. SUBJECT TERMS Partial Ordering, Channel Capcity, Discrete Memory Channel					
16. SECURITY CLASSIFICATION OF:			17. LIMITATION OF ABSTRACT UU	15. NUMBER OF PAGES	19a. NAME OF RESPONSIBLE PERSON Paul Cotae
a. REPORT UU	b. ABSTRACT UU	c. THIS PAGE UU			19b. TELEPHONE NUMBER 202-274-6290

## Report Title

### Partial Ordering and Stochastic Resonance in Discrete Memoryless Channels

#### ABSTRACT

In this thesis, we study the performance of Discrete Memoryless Channels (DMCs) arising in the context of cooperative underwater wireless sensor networks. We introduce a partial ordering for the binary-input ternary output (2,3) DMC. In the particular case of the Binary Symmetric Channel with Symmetric Erasure (BSC/SE), we use majorization theory, channel convexity and directional derivative in order to obtain a partial solution to the open problem of partial ordering of the DMCs. In addition, we analyze the stochastic resonance (SR) phenomenon impact upon the performance limits of a distributed underwater wireless sensor networks operating with limited transmitted power and computational capabilities. We focus on the threshold communication systems where, due to the underwater environment, non-coherent communication techniques are affected both by noise and threshold level. The binary-input ternary-output channel is used as a theoretical model for the DMC. We derived the capacity of the threshold (2,3) DMC in the presence of additive noise. In order to evaluate stochastic resonance, we model the theoretical (2,3) DMC as a physical communication channel corrupted by additive noise with different probability distributions. The (2,3) DMC becomes the BSC/SE when the probability density function of the additive noise is an even function such as Gaussian, Laplace, and Cauchy distribution. Due to the complexity and the non-linearity of the channel capacity analytical expression, the Pinsker and Helgert capacity bounds are also used to evaluate the stochastic resonance in the case of the (2,3) DMC. Our contribution consists in improving the state of the art on the issue of partial ordering for the (2,3) DMC and deriving the optimal noise level required to obtain the maximum capacity for a given threshold decision level in the case of the binary-input ternary-output DMC.

# **Partial Ordering and Stochastic Resonance in Discrete Memoryless Channels**

by

Roland-Yannick Kamdem Kenmogne

A thesis submitted to Graduate Faculty of the  
University of the District of Columbia  
in Partial Fulfillment of the  
Requirements for the Degree of  
Master of Science in  
Electrical Engineering

Washington, DC  
May, 2012

# Partial Ordering and Stochastic Resonance in Discrete Memoryless Channels

Roland-Yannick Kamdem Kenmogne

In this thesis, we study the performance of Discrete Memoryless Channels (DMCs) arising in the context of cooperative underwater wireless sensor networks. We introduce a partial ordering for the binary-input ternary output (2,3) DMC. In the particular case of the Binary Symmetric Channel with Symmetric Erasure (BSC/SE), we use majorization theory, channel convexity and directional derivative in order to obtain a partial solution to the open problem of partial ordering of the DMCs. In addition, we analyze the stochastic resonance (SR) phenomenon impact upon the performance limits of a distributed underwater wireless sensor networks operating with limited transmitted power and computational capabilities. We focus on the threshold communication systems where, due to the underwater environment, non-coherent communication techniques are affected both by noise and threshold level. The binary-input ternary-output channel is used as a theoretical model for the DMC. We derived the capacity of the threshold (2,3) DMC in the presence of additive noise. In order to evaluate stochastic resonance, we model the theoretical (2,3) DMC as a physical communication channel corrupted by additive noise with different probability distributions. The (2,3) DMC becomes the BSC/SE when the probability density function of the additive noise is an even function such as Gaussian, Laplace, and Cauchy distribution. Due to the complexity and the non-linearity of the channel capacity analytical expression, the Pinsker and Helgert capacity bounds are also used to evaluate the stochastic resonance in the case of the (2,3) DMC. Our contribution consists in improving the state of the art on the issue of partial ordering for the (2,3) DMC and deriving the optimal noise level required to obtain the maximum capacity for a given threshold decision level in the case of the binary-input ternary-output DMC.

## **Acknowledgments**

I am thankful to my mentor and advisor Dr. Paul Cotae, P.I. of the Department of Defense (DoD) Research Grant W911NE-11-1-0144, for his guidance and financial support throughout my master study and research.

My sincere thanks go to the Naval Research Laboratory, in particular to Dr. Ira S. Moskowitz for his useful remarks and for his research on top of which my thesis is built.

I would like to acknowledge the Electrical and Computer Engineering Department who has been helpful throughout my master degree, especially Dr. Samuel Lakeou, Dr. Sasan Haghani and Dr. Esther Ososanya.

I am especially thankful to my parents, Esther and Fidel, my sisters, Ginette, Edith, Beryl and my brother, Roland, for their unending support, encouragement and spiritual guidance, my friends, Laetitia, Edema, Garret, and Suresh for their encouragement and stimulating discussion during this research.

Last but not the least I would like to thank God, without whom this would not have been possible.

# Contents

Acknowledgments.....	iii
List of Figures .....	v
List of Abbreviations and Notations.....	vi
Summary .....	vii
Chapter 1 Introduction .....	1
1.1 Thesis Structure .....	1
1.2 Thesis Significance and Contributions .....	2
Chapter 2 Background .....	3
2.1 Communication Channel.....	3
2.1.1 Entropy, Conditional entropy and Joint entropy .....	3
2.1.2 Mutual information and channel capacity.....	4
2.1.3 Example of DMC; binary –input binary-output (2, 2) DMC.....	7
2.2 Partial ordering and DMCs.....	8
2.3 Stochastic Resonance.....	10
Chapter 3 (2,3) DMC Mutual Information and Channel Capacity.....	12
3.1 The general (2,3) DMC .....	12
3.2 Binary Asymmetric Channel with Symmetric Erasure (BAC/SE) .....	13
3.3 Binary Symmetric Channel with Symmetric Erasure (BSC/SE).....	14
3.4 Binary Erasure Channel (BEC) .....	16
3.5 Binary Symmetric Channel (BSC) .....	16
Chapter 4 Partial Ordering of BSC/SE .....	19
4.1 Partial ordering and particular cases .....	20
4.2 Channel convexity and its partial ordering .....	21
Chapter 5 Stochastic Resonance in BSC/SE.....	27
5.1 Physical communication channel and additive noise .....	27
5.2 Stochastic Resonance and additive Gaussian noise.....	32
5.2.1 Stochastic Resonance and Forbidden Interval Theorem in the case of the BSC/SE .....	34
5.2 Stochastic Resonance and capacity bounds for (2, $n$ ) DMC.....	35
5.3 Optimal values for threshold and noise levels.....	38
Chapter 6 Conclusions and future work .....	41
Appendix .....	44

## List of Figures

Figure 1. Communication Channel Model .....	3
Figure 2. Relation between entropy and mutual information.....	4
Figure 3. Gaussian Channel .....	5
Figure 4. (m, n) DMC representation .....	6
Figure 5. Physical communication channel.....	6
Figure 6:( 2, 2) DMC representation .....	7
Figure 7. (2, 2) DMC capacity as a function of $\alpha$ and $\beta$ .....	8
Figure 8. Geometric representation of $A \leq B$ .....	9
Figure 9. SR effect on channel capacity .....	10
Figure 10. (2, 2) DMC Capacity for different values of $\theta = 2, 1.5, 1.1, 1, 0.8, 0.5, 0.3, 0.25$ .....	11
Figure 11. Binary-input ternary output (2,3) DMC .....	12
Figure 12. Binary erasure channel with $p_{11} = 1 - p_{21}$ .....	16
Figure 13. Binary Symmetric Channel.....	16
Figure 14. BSC/SE capacity as a function of $(a, b)$ .....	17
Figure 15. Representation of the BSC/SE in a plane .....	19
Figure 16. Partial ordering of Binary Symmetric Channel Capacity .....	20
Figure 17. Capacity of the Binary Erasure Channel.....	21
Figure 18. BSC/SE Partial Ordering with $a$ and $b$ constants .....	22
Figure 19. BSC/SE partial ordering and directional derivative.....	25
Figure 20. Summary of partial ordering for BSC/SE .....	26
Figure 21. Physical model of binary-input ternary-output communication channel with standard Gaussian noise .....	27
Figure 22. pdf and cdf of the Gaussian noise with $\mu = 0$ and $\sigma = 1$ .....	28
Figure 23. pdf and cdf of Laplace noise with $\mu = 0$ and $\sigma = 2$ .....	29
Figure 24. pdf and cdf of Cauchy noise with location parameter $x_0 = 0$ and scale parameter $\gamma = 1$ .....	30
Figure 25. BAC/SE Capacity C of a threshold system ( $\theta = 2$ ) with three kinds of noise. ....	32
Figure 26. Capacity of BAC/SE as a function of $\theta$ and $\sigma$ .....	33
Figure 27. Capacity of BSC/SE for $\theta = \{0.5, 0.6, 1, 1.5, 2, 2.5, 3, 3.5, 4\}$ .....	33
Figure 28. (2,3) DMC and Pinsker capacity Bound.....	37
Figure 29. (2,3) DMC and Helgert capacity Bound.....	37
Figure 30. Capacity(C), Pinsker (L) and Helgert (U) bounds for different values of $\theta$ .....	38
Figure 31. Optimal noise power and threshold for stochastic resonance, with a scalable factor .....	40

## List of Abbreviations and Notations

AIT	Algebraic Information Theory
AGN	Additive Gaussian Noise
BAC/SE	Binary Asymmetric Channel with Symmetric Erasure
BEC	Binary Erasure Channel
BSC	Binary symmetric Channel
BSC/SE	Binary symmetric Channel with Symmetric Erasure
cdf	Cumulative density function
(m, n)	DMC Discrete Memoryless Channel with m inputs and n outputs
FIT	Forbidden Interval Theorem
i.i.d	Independent and identically distributed
pdf	Probability density function
SR	Stochastic Resonance
$\mathcal{C}(X, Y)$	Channel capacity with input $X$ and output $Y$
$D_{\vec{U}}f(x, y)$	Directional derivatives of a function $f(x, y)$ along the vector $\vec{U}$
$H(f)$	Hessian matrix of a function $f$
$H(X)$	Entropy function of a random variable $X$
$I(X, Y)$	Mutual information of two random variables $X$ and $Y$
$\mathbf{a}$	n-dimensional probability vector
$p_{ij}$	Probability of receiving the message $i$ giving that the message $j$ was sent
$M$	Stochastic Matrix

## Summary

In this thesis, we study the performance of Discrete Memoryless Channels (DMCs) arising in the context of cooperative underwater wireless sensor networks. We introduce a partial ordering for the binary-input ternary output (2,3) DMC. In the particular case of the Binary Symmetric Channel with Symmetric Erasure (BSC/SE), we use majorization theory, channel convexity and directional derivative in order to obtain a partial solution to the open problem of partial ordering of the DMCs. In addition, we analyze the stochastic resonance (SR) phenomenon impact upon the performance limits of a distributed underwater wireless sensor networks operating with limited transmitted power and computational capabilities. We focus on the threshold communication systems where, due to the underwater environment, non-coherent communication techniques are affected both by noise and threshold level. The binary-input ternary-output channel is used as a theoretical model for the DMC. We derived the capacity of the threshold (2,3) DMC in the presence of additive noise. In order to evaluate stochastic resonance, we model the theoretical (2,3) DMC as a physical communication channel corrupted by additive noise with different probability distributions. The (2,3) DMC becomes the BSC/SE when the probability density function of the additive noise is an even function such as Gaussian, Laplace, and Cauchy distribution. Due to the complexity and the non-linearity of the channel capacity analytical expression, the Pinsker and Helgert capacity bounds are also used to evaluate the stochastic resonance in the case of the (2,3) DMC. Our contribution consists in improving the state of the art on the issue of partial ordering for the (2,3) DMC and deriving the optimal noise level required to obtain the maximum capacity for a given threshold decision level in the case of the binary-input ternary-output DMC.

# Chapter 1 Introduction

In this thesis, we discuss the partial ordering and Stochastic Resonance (SR) effect for the binary-input ternary-output (2,3) Discrete Memoryless Channels (DMC). We focus on the Binary Symmetric Channel with Symmetric Erasure (BSC/SE) which is a particular case of the general (2,3) DMC. We establish the relations between the general (2,3) DMC, the Binary Asymmetry Channel with Symmetric Erasure (BAC/SE), the BSC/SE, the Binary Symmetric Channel (BSC) and the Binary Erasure channel (BEC). For the particular case of the BSC/SE, we provide a partial ordering under specific channel noise component constraints using majorization theory, channel convexity and directional derivatives.

In order to study SR, we model the (2,3) DMC by a physical communication channel. In presence of Laplace, Cauchy and Gaussian noise, the SR phenomenon is observed over a certain range of threshold values. We focus on the additive Gaussian noise in which case we determine the interval under which we observe SR. In addition, the Pinsker lower and Helgert upper capacity bounds are used to study SR. The main contributions of this thesis consist in deriving the optimal noise power level required to obtain the maximum capacity for a given threshold decision level and introducing partial ordering for the particular case of the BSC/SE.

## 1.1 Thesis Structure

The rest of the thesis is structured as follows:

**Chapter 2** provides the background concepts and the literature reviews, which will be used throughout the thesis.

**Chapter 3** reviews and derives the mutual information and the capacity of the (2,3) DMC. It also shows the relations between general (2,3) DMC, the binary asymmetric channel with symmetric erasure (BAC/SE), the binary symmetric channel with symmetric erasure (BSC/SE), the binary erasure channel (BER) and the binary symmetric channel (BSC).

**Chapter 4** introduces the partial ordering for the BSC/SE. The partial ordering is based on majorization theory and channel convexity.

**Chapter 5** analyzes the effects of SR and the physical model of the (2,3) DMC in presence of Gaussian, Laplace and Cauchy noise. In addition, the optimal noise level and the optimal threshold level in order to obtain the maximum capacity is derived.

**Chapter 6** engages a discussion about the results and future work.

## 1.2 Thesis Significance and Contributions

This research contributes to Dr. Cotae's research titled "Information - Driven Doppler Shift Estimation and Compensation Methods for Underwater Wireless Sensor Networks", which is to analyze and develop noncoherent communication methods at the physical layer for target tracking and use the information theory tools to predict the next target position by processing the data information collected from a collaborative wireless distributed sensor network [14]. It improves the understanding of the information theory aspects of the physical communication model in the case of (2,3) DMCs. In addition, it contributes to the improvement of the performance limits of distributed underwater wireless sensor networks operating with limited transmitted power and computational environment. The results of this work will contribute to the effort of overcoming the effect of noise in underwater sensors and signal processing.

Precisely, in Chapter 3, we derive the mutual information and the channel capacity of the (2,3) DMC. In Sections 3.1-3.4, the relations between (2,3) DMC, BAC/SE, BSC, and BEC are established. In Chapter 4, Section 4.2, we introduce a partial ordering for the BSC/SE. Three new theorems (Theorems 4.2.1, 4.2.2 and 4.2.3), based on channel convexity and majorization theory, are given and are used to provide a partial ordering for the BSC/SE. In Chapter 5, we evaluate the stochastic resonance phenomenon in the BSC/SE in presence of the additive Gaussian, Laplace, and Cauchy noise. In Section 5.2, we use the Pinsker lower and Helgert upper capacity bounds [13] to evaluate the stochastic resonance phenomenon for the general case of the (2,3) DMC. In section 5.3, the optimal values for the threshold and noise levels resulting in maximum channel capacity are derived.

## Chapter 2 Background

In this chapter, we provide a background review on concepts used throughout the thesis. Mutual information, entropy and channel capacity are reviewed. In addition, we review the current state of the art in partial ordering and stochastic resonance phenomenon of DMC.

### 2.1 Communication Channel

A communication channel, in the Shannon sense [1] is a theoretical model of the physical transmission medium, as shown in Figure 1, which can be used to model a wired or a wireless channel. In this model, the output depends probabilistically on the input. In general, the information associated with a communication channel is characterized by a mutual information function, a joint entropy, a conditional entropy and a channel capacity, defined below.

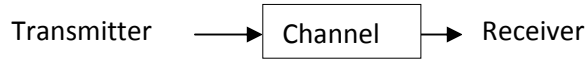


**Figure 1. Communication Channel Model**

#### 2.1.1 Entropy, Conditional entropy and Joint entropy

The entropy,  $H$ , is a measure of uncertainty in a random variable [2]. Mathematically, the entropy is defined as

$$H(X) = -\sum_{x \in X} p(x) \log_2(p(x)) \quad (1)$$

where  $X$  and  $p(x)$  represent a random variable and its probability mass function, respectively. Similar to the entropy, the conditional entropy and joint entropy represent the entropy of a conditional distribution and a joint distribution, respectively. For two random variables  $X$  and  $Y$ , the conditional entropy is defined as

$$H(Y|X) = -\sum_{x,y} p(x,y) \log_2(p(y|x)) \quad (2)$$

and the joint entropy is given by

$$H(X,Y) = -\sum_{x,y} p(x,y) \log_2(p(x,y)) \quad (3)$$

where  $p(x, y)$  and  $p(y|x)$  represent the joint and conditional probability mass function of the random variable  $X$  and  $Y$ , respectively.

### 2.1.2 Mutual information and channel capacity

The mutual information,  $I$ , is a measure of the amount of information one random variable contains about another. It also represents the reduction in uncertainty in a random variable due to another random variable [2]. For two random variables  $X$  and  $Y$ , it is defined by

$$I(X; Y) = H(X) - H(Y|X) \quad (4)$$

From Figure 2, we can easily derive the relations between mutual information, conditional entropy and joint entropy as follow

$$H(X, Y) = H(Y, X) = H(X) + H(Y|X) = H(X|Y) + I(X; Y) + H(Y|X) \quad (5)$$

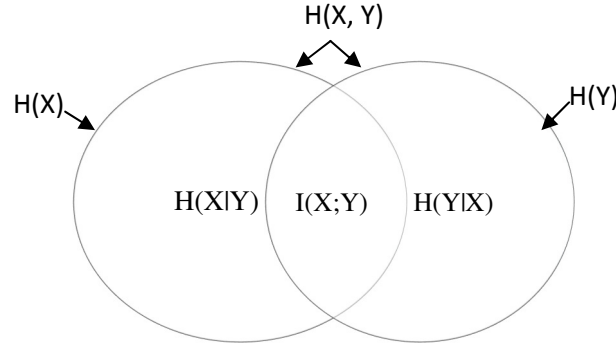


**Figure 2. Relation between entropy and mutual information**

The channel capacity is defined by Shannon [1] as the maximum rate at which one transmits information over the channel and recovers the information at the output with a vanishingly low probability of error. In order to calculate the channel capacity, we maximize the mutual information  $I(X, Y)$  over the input distribution  $p(x), x \in X$ , therefore the capacity can be written as

$$C = \max_{p(x)} I(X; Y) \text{ bits per symbol} \quad (6)$$

where  $X$  and  $Y$  represent the input and output random variable.

Depending on the type of the message transmitted, a communication channel is classified as a continuous or discrete channel. A continuous channel has its transmitted message modeled as continuous signals. The most notorious continuous channel is the Gaussian channel, illustrated in Figure 3, where the output  $Y_i$  at a discrete time  $i$  is the sum of the discrete input  $X_i$  and the continuous noise  $Z_i$ . The sample noise  $Z_i$  is drawn independent identically distributed (i.i.d) from a Gaussian distribution with variance  $\sigma^2$  and zero mean,  $N(0, \sigma^2)$  [2].

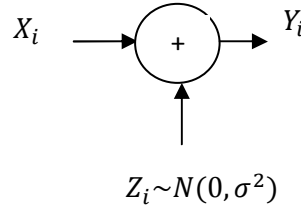


**Figure 3. Gaussian Channel**

The capacity  $C$  of the Gaussian channel with power signal constraint  $P$  and noise variance  $\sigma^2$  is given by

$$C = \frac{1}{2} \log_2 \left( 1 + \frac{P}{\sigma^2} \right) \text{ bits per transmission} \quad (7)$$

Similarly for a Gaussian bandlimited channel we have

$$C = w \log_2 \left( 1 + \frac{P}{\sigma^2 w} \right) \text{ bits per transmission} \quad (8)$$

where  $w$  represents the bandwidth of the channel.

Conversely, a channel is said to be discrete if its transmitted message is modeled as a digital signal as it is depicted in Figure 4.

In this thesis, we focus on the DMC. A discrete channel is said to be memoryless if the constant stationary probability distribution of the output depends only on the input at that time and is conditionally independent of previous channel inputs or outputs [2]. In general, a DMC is

represented by a  $(m, n)$  channel transition probability matrix  $M = \begin{pmatrix} p_{11} & \cdots & p_{n1} \\ \vdots & \ddots & \vdots \\ p_{1m} & \cdots & p_{nm} \end{pmatrix}$ , where each entry  $p_{ji} = p(y_j|x_i)$  represents the conditional probability relation between the output  $y_j$  and the input  $x_i$ .  $M$  is a stochastic matrix.

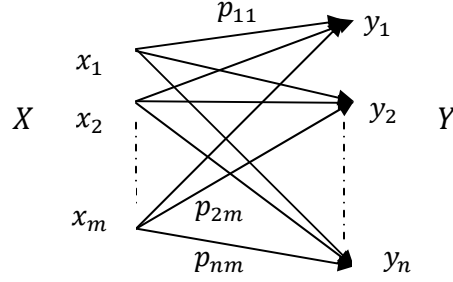


**Figure 4.  $(m, n)$  DMC representation**

In order to study the impact of noise on the channel capacity, we often represent the DMC as a physical communication model as depicted in Figure 5, in which the output is the sum of the additive noise added to the input during the transmission through the channel. The physical communication channel contains a threshold decision block  $t(\theta)$  used to convert the channel output signal  $x_i + n$  into a discrete output  $y_j$ .

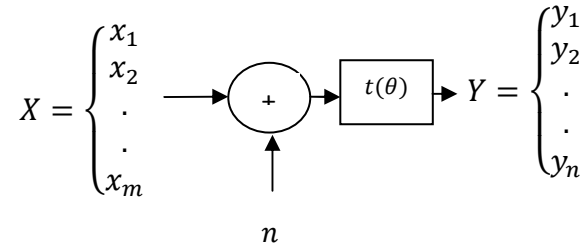


**Figure 5. Physical communication channel**

In [22], an underwater acoustic sensor network with sensors nodes grouped in clusters was proposed. The link between each sensor and the mobile access point is modeled by a DMC. The binary-input binary-output  $(2, 2)$  and binary-input ternary-output  $(2, 3)$  DMCs are of great interest for various digital communications channels, including acoustic underwater communications [3].

### 2.1.3 Example of DMC; binary –input binary-output (2, 2) DMC

The (2, 2) DMC is shown in Figure 6. It is characterized by the input random variable  $X$  and the output random  $Y$  taking values  $(x_1, x_2)$  and  $(y_1, y_2)$ , respectively. Its transition probability matrix is defined by

$$M(\alpha, \beta) = \begin{bmatrix} \alpha & 1 - \alpha \\ \beta & 1 - \beta \end{bmatrix} = \begin{bmatrix} \alpha & \bar{\alpha} \\ \beta & \bar{\beta} \end{bmatrix} \quad (9)$$

where  $\alpha, \beta$  are the conditional probability relationships between the input and the output ( $\alpha = p(Y = y_1|X = x_1), \beta = p(Y = y_2|X = x_2)$ ).

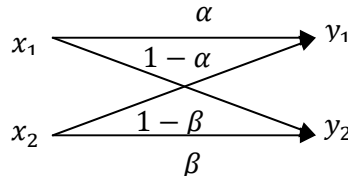


**Figure 6:( 2, 2) DMC representation**

The maximum achievable rate or capacity of the channel  $C$  over different distributions of  $X$  is given by

$$C = \max_{p(x)} I(X; Y) = \max_{p(x_1)} I(X; Y) \quad (10)$$

where  $p(x) = p(x_1) = 1 - p(x_2)$  is the probability of sending the symbol  $x_1$ ,  $p(x_2)$  is the probability of sending the symbol  $x_2$ , and  $I(X, Y)$  is the mutual information between the random variable input  $X$  and output  $Y$ .

In [23], Silverman has shown that the capacity  $C: I^2 \rightarrow [0,1]$ , where  $I^2 = [0,1] \times [0,1]$ , as a function of  $\alpha$  and  $\beta$  is given by

$$C(\alpha, \beta) = \log_2 \left( 2^{\frac{\bar{\alpha}h(\beta) - \bar{\beta}h(\alpha)}{\alpha - \beta}} + 2^{\frac{\beta h(\alpha) - \alpha h(\beta)}{\alpha - \beta}} \right) \quad (11)$$

where  $C(\alpha, \beta) = 0$  if  $\alpha = \beta$  and  $h(x)$  represents the binary entropy function given by

$$h(x) = \begin{cases} -x \log_2(x) - (1-x) \log_2(1-x), & 0 < x < 1 \\ 0, & x = 0, 1 \end{cases}$$

and  $\bar{\alpha} = 1 - \alpha$ .

The capacity of the (2,2) DMC as a function of  $\alpha$  and  $\beta$  is illustrated in Figure 7.

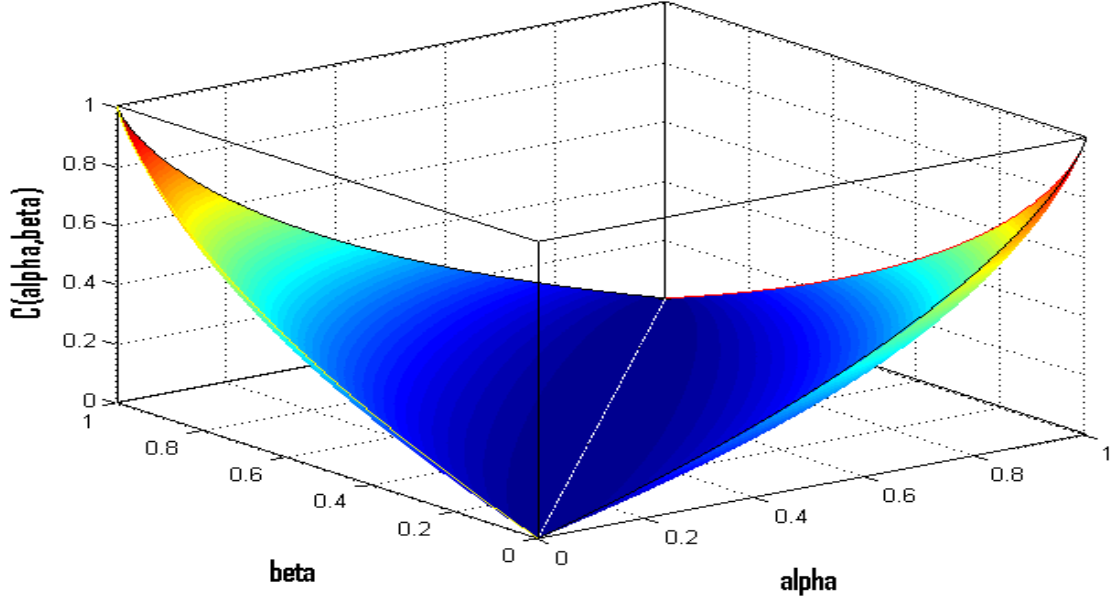


Figure 7. (2, 2) DMC capacity as a function of  $\alpha$  and  $\beta$

## 2.2 Partial ordering and DMCs

The partial ordering of DMC consists of comparing DMC capacity based on the noise components without the computation of the analytical relation of the channel capacity, which in general, is very complex and non-linear. The ordering is critical, especially for wireless sensor communication links at the physical layer operating in very noisy environments with limited computational and power capability [7]. It was first mentioned by Shannon in [24] and later results were developed in [6], [7] and [25] for the (2, 2) DMC.

In [6], the monotonicity principle for convex functions is used to geometrically compare binary DMC capacity. In Figure 8, the set of binary DMCs is represented in the Cartesian plane, where each point representing a channel is located by its coordinate pair  $(\alpha, \beta)$ . Keep in mind

that  $(\alpha, \beta)$  represents the conditional probability relation between the input and output of the channel. The set of positive channels is then defined as the set of all channels such that  $\alpha - \beta = \det(A) \geq 0$ . In [6], it is demonstrated that the (2,2) channel capacity decreases along any line that ends on a zero channel capacity. In order to illustrate the ordering, it is introduced the relation  $\leq$  on the set of positive channels. For two positive binary channels  $A(\alpha, \beta)$  and  $B(c, d)$ , if  $A \leq B$  then  $C(A) \geq C(B)$ , in other terms, the capacity of channel  $A$  is greater than the capacity of channel  $B$ . Geometrically, as depicted in Figure 8, we have  $A \leq B$  if and only if  $B$  is contained in the triangle with vertices  $\{(0,0), (\alpha, \beta), (1,1)\}$ . Analytically  $A \leq B$  iff  $(A = B)$  or  $(\alpha - \beta \geq c - d)$  and  $(1 - c)(\alpha - \beta) \geq (1 - \alpha)(c - d)$ .

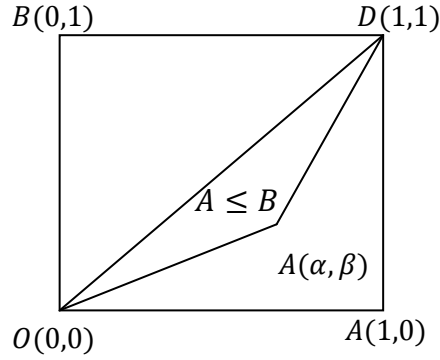


**Figure 8. Geometric representation of  $A \leq B$**

In [7], majorization theory is used to partially order binary DMC under the trace matrix constraint. Cotae and Moskowitz [7] demonstrated that the binary DMC is Schur convex [26] on the region  $R_a$  represented by the triangle ABD and Schur concave on the region  $R_b$  represented by the triangle OAB, as shown in Figure 8. Using these results, they proved that for two binary DMCs,  $(\alpha_1, 1 - \alpha_2) = \begin{pmatrix} \alpha_1 & 1 - \alpha_1 \\ \alpha_2 & 1 - \alpha_2 \end{pmatrix}$  and  $(\beta_1, 1 - \beta_2) = \begin{pmatrix} \beta_1 & 1 - \beta_1 \\ \beta_2 & 1 - \beta_2 \end{pmatrix}$  with the same matrix trace, if  $(\alpha_1, 1 - \alpha_2)$  and  $(\beta_1, 1 - \beta_2) \in R_a$ , and  $(\alpha_1, 1 - \alpha_2)$  is majorized by  $(\beta_1, 1 - \beta_2)$ , then  $C(\alpha_1, 1 - \alpha_2) < C(\beta_1, 1 - \beta_2)$ . On the other hand, if  $(\alpha_1, \alpha_2), (\beta_1, \beta_2) \in R_b$ , then  $C(\alpha_1, 1 - \alpha_2) > C(\beta_1, 1 - \beta_2)$ .

The monotonicity principle and the majorization theory proposed in [6] and [7], respectively, represent an approach and a step forward in solving the open problem of partial ordering.

In this thesis, using the majorization theory, channel convexity and directional derivatives, we extend the results obtained in [6], [7] and [8] for the case of the (2,3) DMC.

### 2.3 Stochastic Resonance

In general, the SR phenomenon is a non-linear effect wherein a communication system can enhance the transmission of the information in the presence of the additive noise [4]. Various performance metrics in the presence of SR such as signal to noise ratio, mutual information, and channel capacity improvement, under a certain range of power noise levels, were discussed in [5]. In Figure 9, the channel capacity is plotted as a function of the noise power level [9]. It is observed that the channel capacity increases, as the noise level increases, until the channel capacity reaches a resonance peak. This increase of the channel capacity is not in concordance with the intuition that increasing the noise power level will decrease the channel capacity.

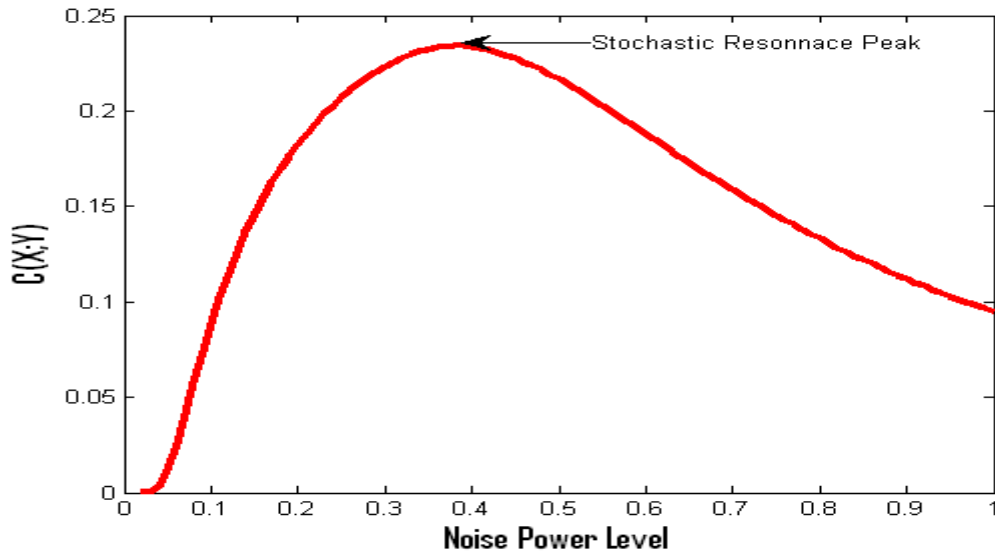
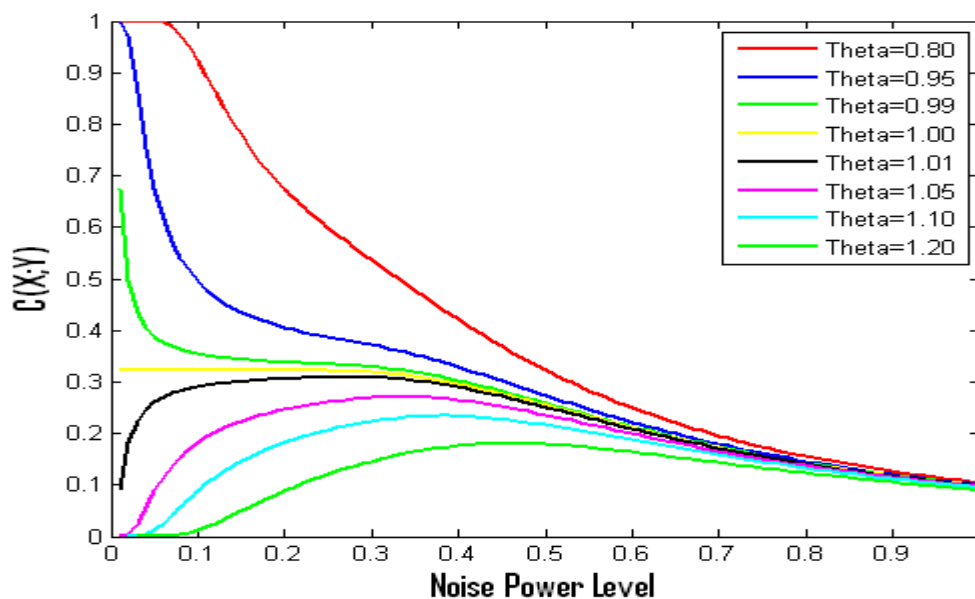


Figure 9. SR effect on channel capacity

In [9] and [10], the SR effect is observed on the binary-input binary-output (2,2) DMC capacity, where maximum channel capacity occurs at an optimal power (variance) of the additive Gaussian noise (AGN) in relation to a given threshold level  $\theta$ , as depicted in Figure 10. In [21],

the Pinsker and Helgert bounds, established in [12], [13], are used to derive the optimal noise power, for a given threshold, that maximize the capacity of the (2,2) DMC.

In this thesis, following Chapeau-Blondeau's work in [5], we analyze the physical communication model of the (2,3) DMC for threshold based SR due to additive noise. Due to the general non-linearity of the DMC capacity, we will use the Pinsker and Helgert capacity bounds to study the capacity behavior of a (2,3) DMC.



**Figure 10. (2, 2) DMC Capacity for different values of  $\theta = \{2, 1.5, 1.1, 1, 0.8, 0.5, 0.3, 0.25\}$**

In this chapter, mutual information, entropy and channel capacity are reviewed. These concepts will be used throughout the remaining of the thesis. In addition, we assessed the current state of the art in partial ordering and stochastic resonance phenomenon of DMC.

## Chapter 3 (2,3) DMC Mutual Information and Channel Capacity

In this chapter, we focus on the general (2,3) DMC and its particular cases. In Section 3.1, we derive the mutual information and capacity of the general (2,3) DMC. In Sections 3.2-3.5, we establish the relations between the general (2,3) DMC, the BAC/SE, the BSC/SE, the BSC, and the BEC.

### 3.1 The general (2,3) DMC

The (2,3) DMC  $\{M: X \rightarrow Y\}$  is characterized by a binary input random variable  $X = \{1, -1\}$ , a ternary output random variable  $Y = \{1, 0, -1\}$ , and a  $(2 \times 3)$  channel transition probability matrix  $M$  defined by  $M = \begin{pmatrix} p_{11} & p_{21} & p_{31} \\ p_{12} & p_{22} & p_{32} \end{pmatrix}$ . The entries of this matrix are the  $p_{ij}$  which represent the conditional probability between each output and input values as represented in Figure 11.

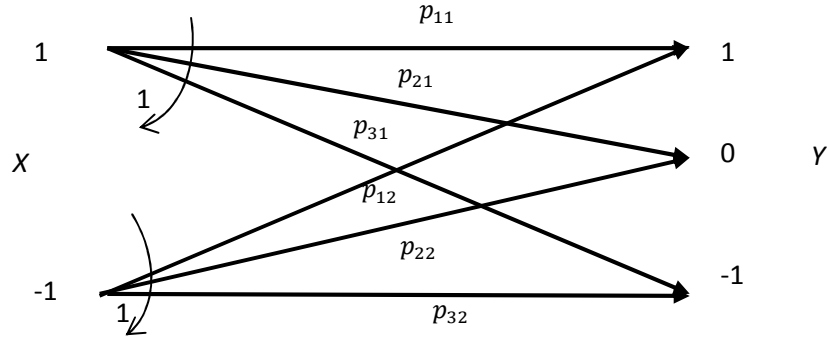


Figure 11. Binary-input ternary output (2,3) DMC

The probability matrix for the (2,3) DMC channel is given by

$M =$

$$\begin{pmatrix} p_{11} = P(Y = 1|X = 1) & p_{21} = P(Y = 0|X = 1) & p_{31} = P(Y = -1|X = 1) \\ p_{12} = P(Y = 1|X = -1) & p_{22} = P(Y = 0|X = -1) & p_{32} = P(Y = -1|X = -1) \end{pmatrix}.$$

Since  $M$  is a stochastic matrix, we have  $p_{31} = 1 - p_{11} - p_{21}$  and  $p_{32} = 1 - p_{12} - p_{22}$ . By defining

$$P(X = i) = p(x_i), \quad i = 1, 2,$$

and

$$P(Y = j) = p(y_j), \quad j = 1, 2, 3,$$

and using (1), (2), and (3) we can rewrite the mutual information as follows

$$I(X, Y) = \sum_{i,j} p(x_i, y_j) \log_2 \frac{p(x_i, y_j)}{p(x_i) \cdot p(y_j)} \quad (12)$$

Since  $p(x_i) \cdot p(y_j|x_i) = p(x_i, y_j)$  and  $p(y_j) = \sum_{k=1}^2 p(y_j|x_k) p(x_k)$  we finally have

$$I(X, Y) = \sum_{i=1}^2 \sum_{j=1}^3 p(x_i) p(y_j|x_i) \log_2 \frac{p(y_j|x_i)}{\sum_{k=1}^2 p(x_k) p(y_j|x_k)} \quad (13)$$

In order to calculate the capacity of the (2,3) DMC channel, we want to maximize the mutual information  $I(X, Y)$ . Based on (13), we observed that  $I(X, Y)$  is a function of  $p(x_1)$  and  $p(x_2)$  since the conditional transition probability  $p(y_j|x_i) = p_{ji}$  is fixed there,  $I(X, Y) = f(p(x_1), p(x_2))$ . Therefore, in order to calculate the capacity of this channel, we need to maximize  $I(X, Y)$  over all distributions of the form  $(p(x_1), p(x_2))$ . Since  $p(x_1) + p(x_2) = 1$ , maximization can only be made over the variable  $x$ , where  $x = p(x_1) = 1 - p(x_2)$ . Therefore, the channel capacity can be written as

$$C = \max_x I(X, Y). \quad (14)$$

Substituting (13) in (14) we obtain

$$C = \max_x \sum_{i=1}^2 \sum_{j=1}^3 p(x_i) p(y_j|x_i) \log_2 \frac{p(y_j|x_i)}{\sum_{k=1}^2 p(x_k) p(y_j|x_k)}. \quad (15)$$

While the general solution for (15) is not known, in [15], a closed form solution is proposed for the capacity of BAC/SE.

### 3.2 Binary Asymmetric Channel with Symmetric Erasure (BAC/SE)

The BAC/SE is a particular case of the (2,3) DMC with the following constraints:  $p_{21} = p_{22}$

and  $p_{11} > p_{12}$ . Its transition probability matrix is given by

$$M = \begin{pmatrix} p_{11} & p_{22} & p_{31} \\ p_{12} & p_{22} & p_{32} \end{pmatrix} \quad (16)$$

In [15], the Kuhn-Tucker condition is used to find the following solution for the BAC/SE channel capacity (See Appendix for the proof):

$$C = \sum_{j=1}^3 p(y_j|x) \log_2 \frac{p(y_j|x)}{x(p(y_j|x_1) - p(y_j|x_2)) + p(y_j|x_2)} \quad \text{for } i = 1, 2 \quad (17)$$

where

$$x = \frac{kp_{32} - p_{12}}{p_{11} - p_{12} - k(p_{31} - p_{32})} \quad (18)$$

and

$$k = \left( \frac{p_{11}^{p_{11}} p_{31}^{p_{31}}}{p_{12}^{p_{12}} p_{32}^{p_{32}}} \right)^{\frac{1}{p_{11} - p_{12}}} \quad (19)$$

Using the closed form solution (16), we will examine the stochastic resonance that arises in the (2,3) BSC/SE channels.

### 3.3 Binary Symmetric Channel with Symmetric Erasure (BSC/SE)

The BSC/SE is a particular case of the BAE/SE with  $p_{11} = p_{32}$ . Since  $M$  is a stochastic matrix, if  $p_{11} = p_{32}$  and  $p_{21} = p_{22}$ , then  $p_{12} = p_{31}$ . Therefore the transition probability matrix of the BSC/SE is given by

$$M = \begin{pmatrix} p_{11} & p_{22} & p_{12} \\ p_{12} & p_{22} & p_{11} \end{pmatrix} \quad (20)$$

We recall from (17) that the capacity of the BAC/SE is given by

$$C = \sum_{j=1}^3 p(y_j|x_j) \log_2 \left( \frac{p(y_j|x_i)}{x(p(y_j|x_1) - p(y_j|x_2)) + p(y_j|x_2)} \right) \quad \text{for } i = 1, 2$$

For example, for  $i = 1$  we have the following expression

$$C = p_{11} \log_2 \frac{p_{11}}{x(p_{11}-p_{12})+p_{12}} + p_{21} \log_2 \frac{p_{21}}{x(p_{21}-p_{22})+p_{22}} + p_{31} \log_2 \frac{p_{31}}{x(p_{31}-p_{32})+p_{32}} \quad (21)$$

Using the following equalities  $p_{11} = p_{32}$  and  $p_{22} = p_{21}$ , the capacity simplifies to

$$C = p_{11} \log_2 \frac{p_{11}}{x(p_{11}-p_{12})+p_{12}} + p_{31} \log_2 \frac{p_{31}}{x(p_{31}-p_{32})+p_{32}} \quad (22)$$

We will determine the value of  $x$  that maximizes the mutual information of the BSC/SE. From (18) and (19) we have

$$x = \frac{kp_{32}-p_{12}}{p_{11}-p_{12}-k(p_{31}-p_{32})} \quad \text{with} \quad k = \left( \frac{p_{11}p_{11}p_{31}p_{31}}{p_{12}p_{12}p_{32}p_{32}} \right)^{\frac{1}{p_{11}-p_{12}}}$$

Using the previous constraints, when applied to the BSC/SE  $p_{12} = p_{31}$  and  $p_{21} = p_{22}$  and  $p_{11} = p_{32}$ , we have

$$k = 1 \quad \text{and} \quad x = \frac{p_{32}-p_{32}}{2(p_{11}-p_{32})} = \frac{1}{2} \quad (23)$$

Therefore (22) becomes

$$C = p_{11} \log_2 \frac{2p_{11}}{p_{11}+p_{31}} + p_{31} \log_2 \frac{p_{31}}{p_{11}+p_{31}} \quad (24)$$

It is interesting to note that the capacity of the BSC/SE is function only of two variables just as in the (2, 2) DMC. If we set  $p_{11} = a$ ,  $p_{31} = b$ ,  $c = p_{12}$  and  $d = p_{32}$  then we can re-write both  $M$  and  $C(X, Y)$  for the particular case of the BSC/SE as follows

$$M = \begin{pmatrix} a & 1-a-b & b \\ b & 1-a-b & a \end{pmatrix}$$

and

$$C(a, b) = a \log_2 \frac{2a}{a+b} + b \log_2 \frac{2b}{a+b} \quad (25)$$

With  $1 \geq a, b \geq 0$  and  $a + b \leq 1$ .

Next, we will focus on the binary erasure channel.

### 3.4 Binary Erasure Channel (BEC)

The BEC, shown in Figure 12, is a particular case of the BSC/SE with the particularity that  $p_{12} = p_{31} = 0$ . Replacing  $p_{12} = p_{31} = 0$  in (25) the capacity of the BEC becomes

$$C = p_{11} \log_2 \frac{2p_{11}}{p_{11}} = p_{11} = 1 - p_{21} \quad (26)$$

which corresponds to the well-known capacity of the binary erasure channel [2]. For  $i = 2$  in (19), following the same steps, we obtain the same result for  $C$ .

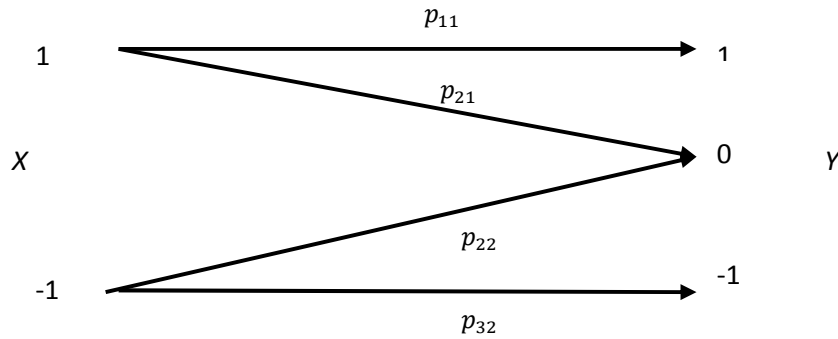


Figure 12. Binary erasure channel with  $p_{11} = 1 - p_{21}$

### 3.5 Binary Symmetric Channel (BSC)

The BSC, depicted in Figure 13, is a particular case of the (2, 2) DMC but can also be derived from the BSC/SE when  $p_{21} = p_{22} = 0$ .

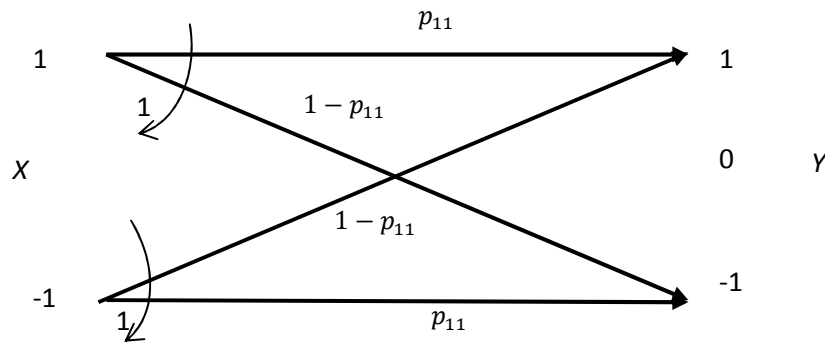


Figure 13. Binary Symmetric Channel

*Proof:* Given that  $M$  is a stochastic matrix, if  $p_{21} = p_{22} = 0$  then  $p_{31} = 1 - p_{11}$ , therefore replacing  $p_{31} = 1 - p_{11}$  in (24), we have

$$C = p_{11} \log_2 2p_{11} + (1 - p_{11}) \log_2 2(1 - p_{11}) \quad (27)$$

$$= \log_2 (2p_{11})^{p_{11}} + \log_2 (2(1 - p_{11}))^{1-p_{11}}$$

$$= \log_2 (2p_{11}^{p_{11}} (1 - p_{11})^{1-p_{11}}), \text{ so}$$

$$C = 1 - (-p_{11} \log_2 (p_{11}) - (1 - p_{11}) \log_2 (1 - p_{11})) = 1 - H(p_{11}) \quad (28)$$

The above relation corresponds to the channel capacity of the BSC.

In Figure 14, we plot the BSC/SE (25) in function of the noise elements  $a$  and  $b$ . In the same Figure, we illustrate the BSC, which occurs when  $a = 1 - b$  and the BEC, which occurs when  $b = 0$ .

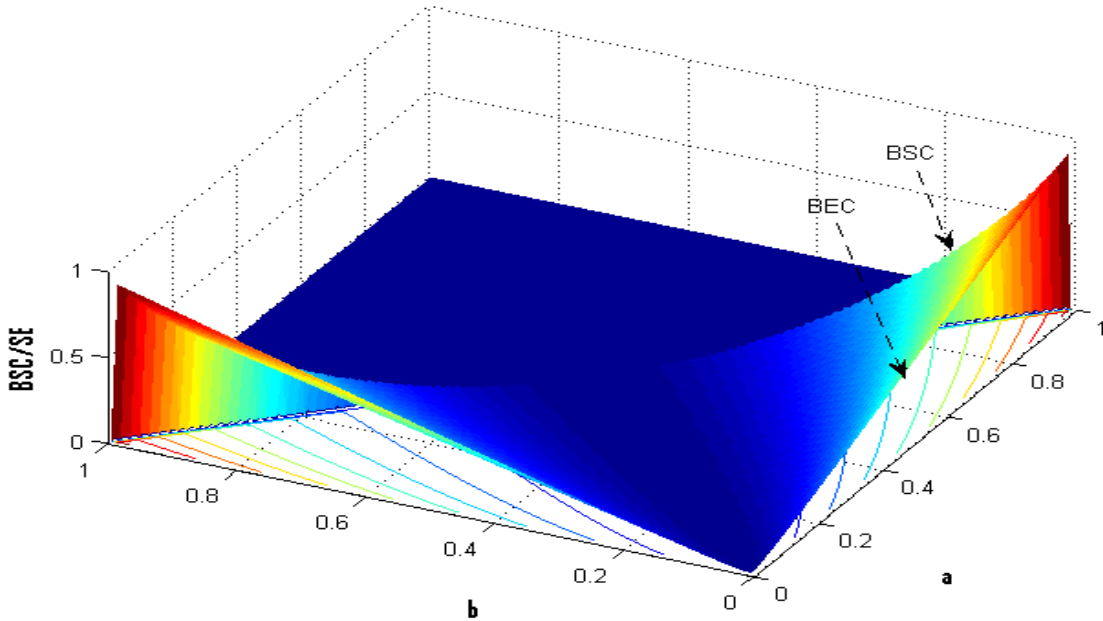


**Figure 14.** BSC/SE capacity as a function of  $(a, b)$

In summary, we have derived the mutual information and the channel capacity of the general (2,3) DMC. In addition, the solution of the capacity of the BAC/SE is used to establish the relationships between the BAC/SE, the BSC/SE, the BSC, and the BEC. We proved that the BSC and the BEC are all particular cases of the general (2,3) DMC. The results of this chapter are summarized in Table.1.

**Table 1: Summary of (2,3) DMCs**

Channel	$M$	Constraints	Channel Capacity
(2,3) general DMC	$\begin{pmatrix} a & 1-a-b & b \\ c & 1-c-d & d \end{pmatrix}$		
BAC/SE	$\begin{pmatrix} a & 1-a-b & b \\ c & 1-c-d & d \end{pmatrix}$	$\begin{aligned} a &> b \\ 1-a-b \\ &= 1-c \\ &-d \end{aligned}$	$\sum_{j=1}^3 p(y_j x_j) \log_2 \left( \frac{p(y_j x_i)}{x(p(y_j x_1) - p(y_j x_2)) + p(y_j x_2)} \right)$
BSC/SE	$\begin{pmatrix} a & 1-a-b & b \\ c & 1-c-d & d \end{pmatrix}$	$\begin{aligned} a &> b \\ a &= d \\ b &= c \end{aligned}$	$a \log_2 \frac{2a}{a+b} + b \log_2 \frac{2b}{a+b}$
BSC	$\begin{pmatrix} a & 1-a-b & b \\ c & 1-c-d & d \end{pmatrix}$ $\equiv \begin{pmatrix} a & 1-a \\ 1-a & a \end{pmatrix}$	$\begin{aligned} a+b &= 1 \\ a &= d \\ b &= c \end{aligned}$	$1 - h(a)$
BEC	$\begin{pmatrix} a & 1-a & 0 \\ 0 & 1-a & 0 \end{pmatrix}$	$\begin{aligned} b &= c \\ &= 0 \\ a &= d \end{aligned}$	$a$

## Chapter 4 Partial Ordering of BSC/SE

In this section, we focus on partial ordering in the case of the BSC/SE. The BSC/SE is of interest because in [16], it is proven that in presence of additive Gaussian noise (AGN), the general (2,3) channel becomes the BSC/SE (2,3). Our partial ordering is based on channel convexity and majorization theory [26]. In Section 4.1, we review the partial ordering for the particular case of the BSC and BEC. In Section 4.2, we prove three theorems (Theorems 4.2.1, 4.2.2 and 4.2.3) based on channel convexity and majorization theory. These theorems are used to provide a partial ordering for the BSC/SE.

We recall from (25) that  $C(a, b) = a \log_2 \frac{2a}{a+b} + b \log_2 \frac{2b}{a+b}$  with  $1 \geq a, b \geq 0$  and,  $a + b \leq 1$ ; we will, given the noises resources  $a$  and  $b$ , determine the channel with the higher capacity without computing (25) or using the Moskowitz approximations [12].

In Figure 15, we represent the set of BSC/SEs in the Cartesian plane. The capacity expression of the BSC/SE is defined over the triangle  $OAB$ . The triangle  $OAB$  corresponds to the constraints that apply to the noise elements  $a$  and  $b$ , that is,  $0 \leq a, b \leq 1$  and  $a + b \leq 1$ . Using (25), we can easily verify  $C(a, b) = C(b, a)$ . Note that along the AC segment ( $y = x$ ), the BSC/SE capacity is null (zero channel capacity). Similar along the OA segment we have the BEC and along the AB segment we have the BSC ( $y = 1 - x$ ). In Figure 15, the points  $A(1,0)$  and  $B(0,1)$  represent the noiseless BSC/SE channel.

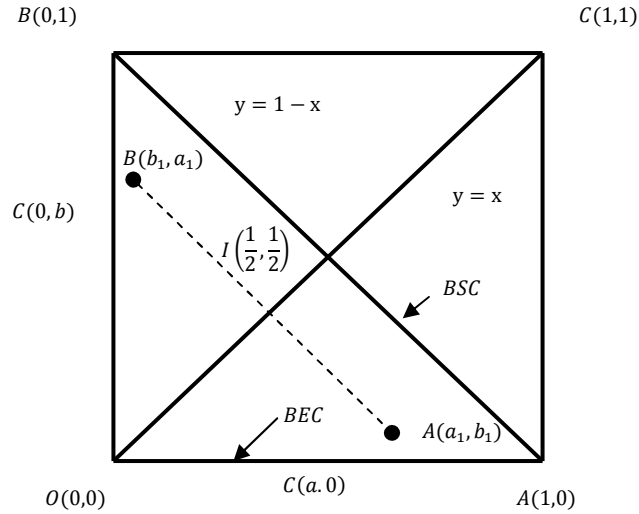


Figure 15. Representation of the BSC/SE in a plane

#### 4.1 Partial ordering and particular cases

In [7], a partial ordering for the BSC was proposed. For a BSC with a crossover probability  $a$  and a transition matrix  $M = \begin{pmatrix} a & 1-a \\ 1-a & a \end{pmatrix}$ , when  $a > \frac{1}{2}$  and  $a$  is increasing, the capacity is increasing with a minimum capacity of 0 bits per transmission (zero channel capacity  $a = \frac{1}{2}$ ) and a maximum of 1 bit per transmission (noiseless channel  $a = 1$ ). By symmetry, when  $a < \frac{1}{2}$  and  $a$  is decreasing, the capacity of the BSC is also increasing with a minimum capacity of 0 bits per transmission (zero channel capacity  $a = \frac{1}{2}$ ) and a maximum of 1 bit per transmission (noiseless channel  $a = 1$ ). Therefore in order to partially order BSCs, all one needs is to compare the crossover probability. For two BSCs with crossover probability  $a_1$  and  $a_2$ , if  $a_1 > a_2 > \frac{1}{2}$ , then  $C(a_1, 1 - a_1) > C(a_2, 1 - a_2)$ , as depicted in Figure 16, similarly, if  $a_1 < a_2 < \frac{1}{2}$  then  $C(a_1, 1 - a_1) > C(a_2, 1 - a_2)$ .

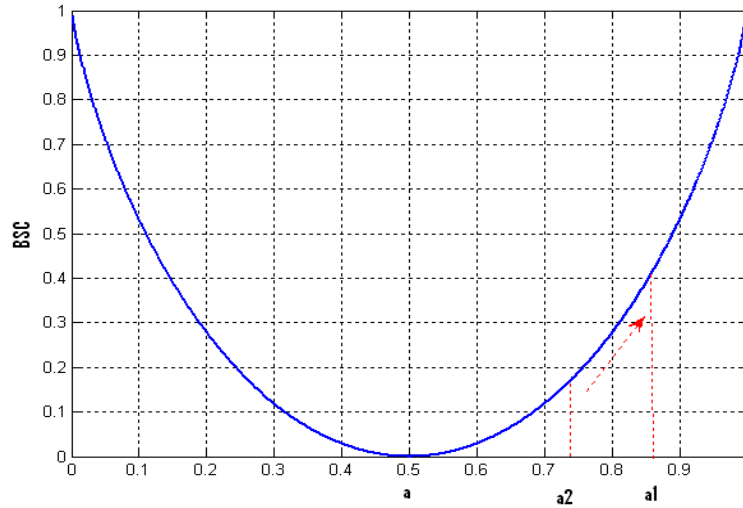
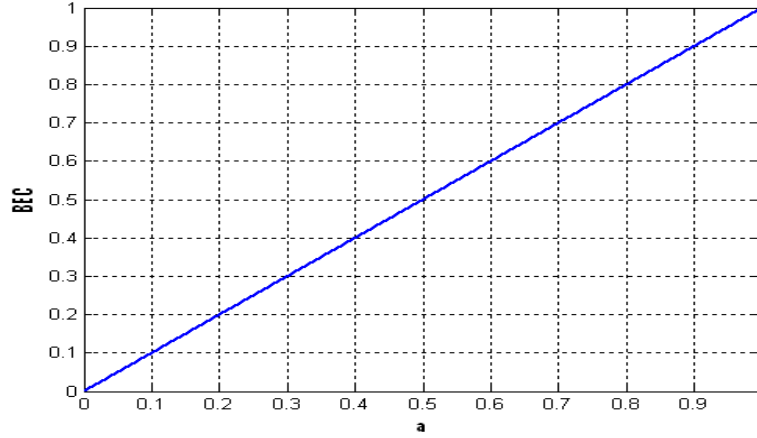


Figure 16. Partial ordering of Binary Symmetric Channel Capacity

For the BEC with a probability of erasure  $1 - a$  and a transition matrix  $M = \begin{pmatrix} a & 1-a & 0 \\ 0 & 1-a & 0 \end{pmatrix}$ , the capacity of the BEC is an increasing function of  $a$  as depicted in Figure 17. Therefore for two BECs with probabilities of erasure  $1 - a_1$  and  $1 - a_2$ , if  $a_1 > a_2$ , then  $C(a_1, 1 - a_1) > C(a_2, 1 - a_2)$ .



**Figure 17. Capacity of the Binary Erasure Channel**

#### 4.2 Channel convexity and its partial ordering

Our approach of partial ordering is based on partial derivatives, channel convexity and majorization theory. We will focus in the  $OIA$  triangle, shown in Figure 15. The partial ordering is done under each of the following constraints on the noise elements:  $a$  is constant,  $b$  is constant,  $a + b$  is constant, and  $a - b$  is constant. The same result could be applied to the channel capacity in the  $OIB$  triangle because of the symmetry of the BSC/SE. We introduce the following theorems.

Theorem 4.2.1: For BSC/SEs defined by the transition probability matrix  $M_i = \begin{pmatrix} a_i & 1 - a_i - b_i & b_i \\ b_i & 1 - a_i - b_i & a_i \end{pmatrix}$ ,  $i = 1, 2$ , if  $a_i$  is constant, and  $b_1 > b_2$ , then  $C(a_i, b_1) < C(a_i, b_2)$ . Conversely if  $b_i$  is constant and  $a_1 > a_2$ , then  $C(a_1, b_i) > C(a_2, b_i)$ .

*Proof:* In order to prove the above theorem we will find the partial derivatives of the channel capacity. We have

$$\begin{aligned} \frac{\partial C(a, b)}{\partial a} &= \frac{\partial}{\partial a} \left( a \log_2 \frac{2a}{a+b} + b \log_2 \frac{2b}{a+b} \right) \\ &= \frac{b}{a+b} - \frac{b}{a+b} + \log_2 \left( \frac{2a}{a+b} \right) \end{aligned}$$

$$= \log_2 \left( \frac{2a}{a+b} \right).$$

Given that we are in the  $OIA$  triangle, we have  $a > b$  or  $2a > a + b$  which imply that

$$\frac{\partial C(a,b)}{\partial a} > 0,$$

so for any fixed  $b$ , the function  $C(a,b)$  is strictly increasing; therefore for  $b = \text{constant}$ , if  $a_1 > a_2$  then  $C(a_1, b) > C(a_2, b)$ . Similarly, we have

$$\frac{\partial C(a,b)}{\partial b} = \log_2 \left( \frac{2b}{a+b} \right) < 0,$$

therefore for a fixed  $a$  the function  $C(a,b)$  is strictly decreasing, therefore for  $a = \text{constant}$ , if  $b_1 > b_2$  then  $C(a, b_1) < C(a, b_2)$ .

The above theorem is summarized in Figure 18. For any BSC/SE  $(a_i, b_i)$  included in the polygon formed by the intersection of the horizontal and vertical segment from  $(a_1, b_1)$  to both the  $y = x$  line (for  $a < \frac{1}{2}$ ) or the  $y = x$  line and the  $y = 1 - x$  line (for  $a > \frac{1}{2}$ ),  $C(a_i, b_i) < C(a_1, b_1)$ .

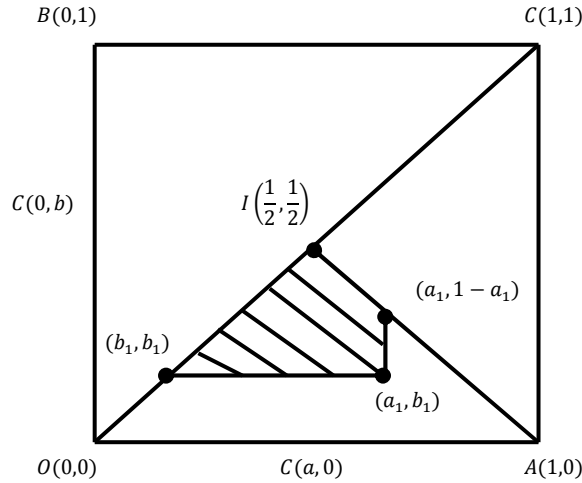


**Figure 18. BSC/SE Partial Ordering with  $a$  and  $b$  constants**

From these results, the partial ordering is done as follows; given two BSC/SE transition stochastic matrices  $M_i = \begin{pmatrix} a_i & 1 - a_i - b_i & b_i \\ b_i & 1 - a_i - b_i & a_i \end{pmatrix}$  and  $M_1 = \begin{pmatrix} a_1 & 1 - a_1 - b_1 & b_1 \\ b_1 & 1 - a_1 - b_1 & a_1 \end{pmatrix}$ , if  $a_i < a_1$  and  $b_i > b_1$  then  $C(a_i, b_i) < C(a_1, b_1)$ .

The next partial ordering theorem is based on channel convexity, directional derivative and majorization theory.

Definition 4.2.1:[27] A function  $f(x_1, x_2, \dots, x_n)$  is convex if its  $(n \times n)$  Hessian matrix

$$H(f) = \begin{pmatrix} \frac{\partial^2 f}{\partial x_1^2} & \dots & \frac{\partial^2 f}{\partial x_1 \partial x_n} \\ \vdots & \ddots & \vdots \\ \frac{\partial^2 f}{\partial x_n \partial x_1} & \dots & \frac{\partial^2 f}{\partial x_n^2} \end{pmatrix} \text{ is positive semidefinite; that, is the eigenvalues of the } H(f)$$

matrix are non-negative.

Theorem 4.2.2: The BSC/SE is a convex function.

*Proof:* Based on Def 4.2.1 we will obtain the Hessian matrix of the BSC/SE and compute its eigenvalues. We have

$$\begin{aligned} \frac{\partial^2 C(a,b)}{\partial a^2} &= \frac{b}{a^2+ab} & \text{and} & & \frac{\partial^2 C(a,b)}{\partial b^2} &= \frac{a}{b^2+ab} \\ \frac{\partial^2 C(a,b)}{\partial a \partial b} &= \frac{-1}{a+b} & \text{and} & & \frac{\partial^2 C(a,b)}{\partial b \partial a} &= \frac{-1}{a+b} \end{aligned}$$

Therefore

$$H(C) = \frac{1}{\log_{10}(2)} \begin{pmatrix} \frac{b}{a^2+ab} & -\frac{1}{a+b} \\ -\frac{1}{a+b} & \frac{a}{b^2+ab} \end{pmatrix} \quad (29)$$

and the eigenvalues of  $H(C)$  are

$$\lambda = 0 \text{ and } \lambda = \frac{a^2+b^2}{ab(a+b)\log(2)} \geq 0 \quad (30)$$

Therefore the BSC/SE is a convex function. This motivates using majorization theory for partial ordering of (2,3) BSC/SE.

Definition 4.2.2: [26] A real-value function  $\phi$  defined on the set of n-dimensional probability vectors is said to be Shur convex (Shur Concave) if  $\phi$  is order preserving (inverse order preserving) with respect to the partial order  $<$ . That is if

$$\mathbf{a} < \mathbf{b} \Rightarrow \phi(\mathbf{a}) < \phi(\mathbf{b}) \quad (\mathbf{a} < \mathbf{b} \Rightarrow \phi(\mathbf{a}) > \phi(\mathbf{b})) \quad (31)$$

Definition 4.2.3: [27] The directional derivative  $D_{\vec{u}}f(x,y)$ , of a multivariate differentiable function  $f_x(x,y)$  along a given unit vector  $\vec{u}$  at a given point  $(x,y)$  represents the instantaneous rate of change of the function moving through  $(x,y)$  in the direction of  $\vec{u}$ .

$$D_{\vec{u}}f(x,y) = e_1 \frac{\partial f(x,y)}{\partial x} + e_2 \frac{\partial f(x,y)}{\partial y} \quad (32)$$

where  $\vec{u}(e_1, e_2)$  is a unit vector [27].

We will re-write (25) as

$$C(x,y) = x \log_2 \frac{2x}{x+y} + y \log_2 \frac{2y}{x+y} \quad (33)$$

in the  $(0, x, y, z)$  Euclidian 3-space where  $1 \geq x \geq y \geq 0$  and  $x + y \leq 1$ . We define the region  $R_G$ , constituted of the set  $(x,y)$ , such that,  $1 \geq x \geq y \geq 0$  and  $x + y \leq 1$

Theorem 4.2.3: For BSC/SEs defined by the transition probability matrix  $M_i = \begin{pmatrix} a_i & 1 - a_i - b_i & b_i \\ b_i & 1 - a_i - b_i & b_i \end{pmatrix}$ ,  $i = 1, 2, \dots$ , if  $a_i + b_i$  is constant then the capacity function of the BSC/SE is Schur convex.

*Proof:* Our proof is based on directional derivative. One can easily prove using vector calculus that for any two points  $(x_1, k - x_1)$  and  $(x_2, k - x_2) \in R_G$ , such that  $x_1 > x_2$ , the unit vector of the line  $x + y = k$  is  $\vec{u}(-\frac{1}{\sqrt{2}}, \frac{1}{\sqrt{2}})$ . Similarly, if  $(x_1 < x_2)$ , then the unit vector along the line

$x + y = k$  is  $\vec{u}'(\frac{1}{\sqrt{2}}, -\frac{1}{\sqrt{2}})$ . Therefore the directional derivative of  $C(x, y)$  along  $\vec{u}$  at any given point  $(x, y)$  is given by

$$D_{\vec{u}}C(x, y) = \frac{1}{\sqrt{2}} \log_2 \left( \frac{y}{x} \right) < 0 \quad (34)$$

From (34), we can conclude that the capacity decreases along any line of equation  $x + y = k$  in the direction of  $\vec{u}$ . In other terms, for any two points  $(x_1, y_1)$  and  $(x_2, y_2)$  such that  $x_1 + y_1 = x_2 + y_2$  and  $x_1 > x_2$ , that is, if  $(x_1, y_1) \succ (x_2, y_2)$ , then  $C(x_1, y_1) > C(x_2, y_2)$ . This proves that, if  $x + y$  is constant, then the capacity is Shur-convex.

By defining  $\vec{v}(\frac{1}{\sqrt{2}}, \frac{1}{\sqrt{2}})$ , as the unit vector of the line  $x - y = k$ , the previous approach could be used to prove the following theorem:

**Theorem 4.2.4:** For any  $(x_1, y_1), (x_2, y_2) \in R_G$  such that  $x_1 - y_1 = x_2 - y_2$  if  $x_1 < x_2$ , then  $C(x_1, y_1) > C(x_2, y_2)$ .

Theorems 4.2.3 and 4.2.4 are summarized in Figure 19, where the capacity decreases in either direction of  $\vec{u}$  or  $\vec{v}$ .

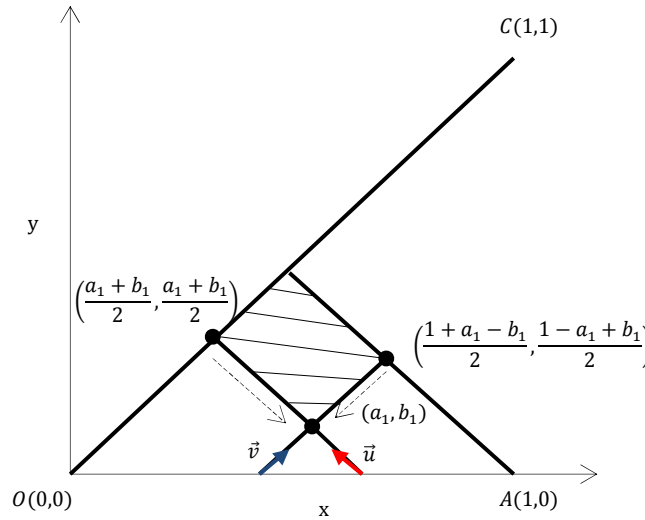
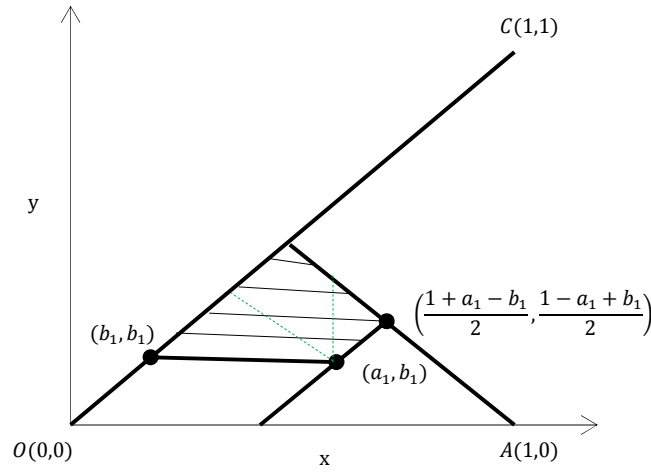


Figure 19. BSC/SE partial ordering and directional derivative

The results from Theorem 4.2.1, 4.2.3 and 4.2.4 are represented in Figure 20. These results improve the partial ordering previously discussed. For any  $(a_i, b_i)$  includes in the polygon, as shown in Figure 20, with vertices  $\{(a_1, b_1), (\frac{1+a_1-b_1}{2}, \frac{1-a_1+b_1}{2}), (\frac{1}{2}, \frac{1}{2}), (b_1, b_1)\}$ ,  $C(a_1, b_1) \geq C(a_i, b_i)$ . Analytically this translates into

$$\text{If } \begin{cases} a_i < \frac{1+a_1-b_1}{2} \\ b_i > b_1 \\ a_i - b_i < a_1 - b_1 \end{cases} \text{ then } C(a_1, b_1) \geq C(a_i, b_i) \quad (35)$$



**Figure 20. Summary of partial ordering for BSC/SE**

*Example:* Consider two BSC/SEs with respective noise matrices  $A = \begin{pmatrix} 0.6 & 0.1 & 0.2 \\ 0.2 & 0.1 & 0.6 \end{pmatrix}$  and

$B = \begin{pmatrix} 0.5 & 0.2 & 0.3 \\ 0.3 & 0.2 & 0.5 \end{pmatrix}$ . Which channel has the highest capacity?

We have  $0.6 > 0.5$  and  $0.2 < 0.3$ ; therefore without computing (27), we have  $C(A) > C(B)$ .

In conclusion, this chapter provides a partial ordering for BSC/SE under several noise component constraints  $a$  and  $b$ , which represents the conditional probability relationships between the inputs and the outputs of the channel. We partially order BSC/SE when  $a$  or  $b$  is constant. In addition, we prove that when  $a + b$  is constant, the capacity function of the BSC/SE is Schur-convex for which case we use majorization theory to partially order BSC/SE.

## Chapter 5 Stochastic Resonance in BSC/SE

In this chapter, following the work of [17], we examine the effect of additive Gaussian noise, Laplace noise, and Cauchy noise on the capacity of the (2,3) BSC/SE derived in (25). We assume that noise has a Gaussian, Laplace, and Cauchy distribution, all with zero mean (zero location parameter for Cauchy distribution). The physical communication channel is used to model the (2,3) DMC and to derive the probability transition matrix components  $p_{ij}$  of the (2,3) DMC in presence of the Gaussian, Laplace, and Cauchy noise. The SR is observed for the (2,3) DMC in presence of Gaussian, Laplace, and Cauchy noise. In Section 5.1, we focus on the particular case of the AGN, for which case we use theorems derived in Section 4.2 to determine the forbidden interval [20] of the BSC/SE capacity. In Section 5.2, the Pinsker lower and Helgert upper capacity bounds are used to evaluate the SR in the BSC/SE. In Section 5.3, the optimum threshold value that maximizes the channel capacity of the BSC/SE is derived.

### 5.1 Physical communication channel and additive noise

The physical model is represented in Figure 21, where in the presence of the additive noise  $n$ , and the input signal  $s$ , the received signal  $y$  is given by

$$y = s + n \quad (36)$$

The input  $s$  takes the binary values of -1 and 1, with the probabilities  $p(s_1) = p(s = -1)$  and  $p(s_2) = p(s = 1)$ .

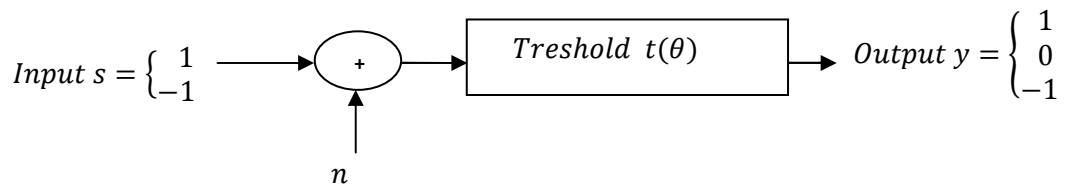


**Figure 21. Physical model of binary-input ternary-output communication channel  
with standard Gaussian noise**

The physical communication channel contains a threshold decision block function  $t(\theta)$ , where  $\theta$  represents the threshold value. Based on the threshold level  $\theta$  and the noise level, the received signal is converted into a discrete random variable  $y$  taking on the values of 1, 0, or -1.

For the ternary output, the threshold function is defined as follows:

$$t(\theta) = \begin{cases} -1 & s + n < -\theta \\ 0 & -\theta \leq s + n \leq \theta \\ 1 & s + n > \theta \end{cases} \quad (37)$$

By using the threshold level, the analytic expression for each of the conditional probabilities  $p_{11}$ ,  $p_{21}$ ,  $p_{31}$ ,  $p_{12}$ ,  $p_{22}$ ,  $p_{32}$  between the binary input and the ternary output in presence of additive Gaussian, Laplace, and Cauchy noise will be determined.

We start by giving a brief review of the pdf and the cdf of the Gaussian, Laplace and Cauchy noise.

- **Gaussian Noise:** The Gaussian noise with mean  $\mu = 0$  and variance  $\sigma > 0$  has the following probability density function and cumulative density distribution, respectively. In Figure 22, we plot the pdf and the cdf for Gaussian noise with  $\mu = 0$  and  $\sigma = 1$ .

$$f(n) = \frac{1}{\sigma\sqrt{2\pi}} e^{-\frac{n^2}{2\sigma^2}} \quad (38)$$

$$F_n(\theta) = P_r(n \leq \theta) = \frac{1}{\sigma\sqrt{2\pi}} \int_{-\infty}^{\theta} e^{-\frac{t^2}{2\sigma^2}} dt \quad (39)$$

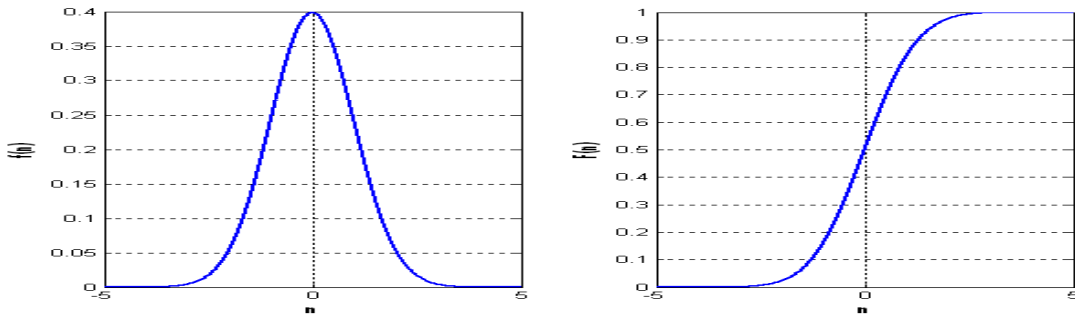


Figure 22. pdf and cdf of the Gaussian noise with  $\mu = 0$  and  $\sigma = 1$

- **Laplace noise:** Laplace noise with  $\mu = 0$  and variance  $\sigma = 2\beta^2$  has the following probability density function and cumulative density distribution, respectively. In Figure 24, we plot the pdf and the cdf for Laplace noise with  $\mu = 0$  and  $\sigma = 2$ .

$$f(n) = \frac{1}{2\beta} e^{-\frac{|n|}{\beta}} \quad (40)$$

$$F_n(\theta) = P_r(n \leq \theta) = \begin{cases} \frac{1}{2} e^{\frac{\theta}{\beta}} & \theta < 0 \\ 1 - \frac{1}{2} e^{-\frac{\theta}{\beta}} & \theta \geq 0 \end{cases} \quad (41)$$

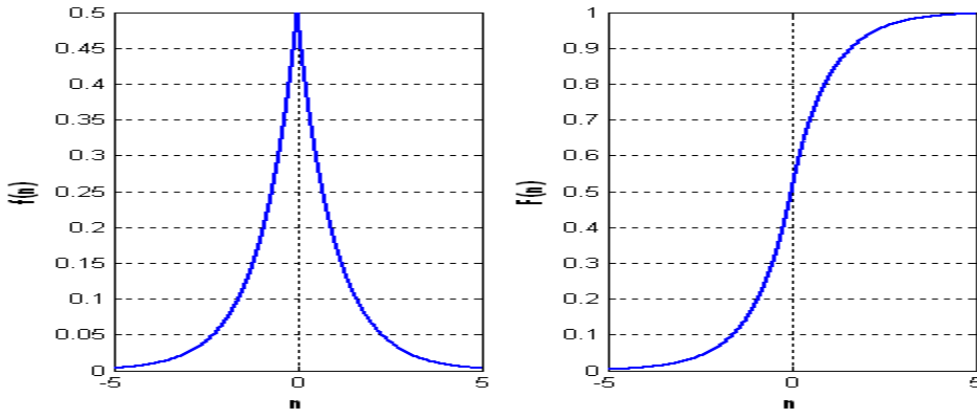
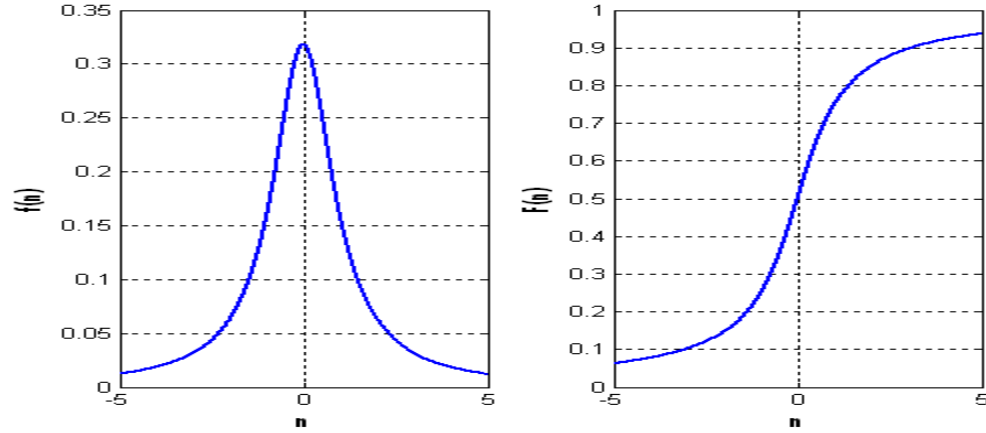


Figure 23. pdf and cdf of Laplace noise with  $\mu = 0$  and  $\sigma = 2$

- **Cauchy noise:** The Cauchy noise with location parameter  $x_0 = 0$  and scale parameter  $\gamma$  has the following probability density function and cumulative density distribution respectively. In Figure 24, we plot the pdf and the cdf for Gaussian noise with  $x_0 = 0$  and  $\gamma = 1$

$$f(n) = \frac{1}{\pi} \frac{\gamma}{n^2 + \gamma^2} \quad (42)$$

$$F_n(\theta) = \frac{1}{\pi} \arctan\left(\frac{\theta}{\gamma}\right) + \frac{1}{2} \quad (43)$$



**Figure 24. pdf and cdf of Cauchy noise with location parameter  $x_0 = 0$  and scale parameter  $\gamma = 1$**

The following results are valid for any of the distributions described above.

Following the physical model depicted in Figure 21, we have

$$p_{11} = P(1|1) = P(Y = 1|S = 1) = \Pr(s + n > \theta | s = 1) = 1 - \Pr(n < -1 + \theta) = 1 - F_n(-1 + \theta) \quad (44)$$

Using a similar approach we have

$$\begin{cases} p_{21} = P(0|1) = F_n(-1 + \theta) - F_n(-1 - \theta) \\ p_{31} = P(-1|1) = F_n(-1 - \theta) \\ p_{12} = P(1|-1) = 1 - F_n(1 + \theta) \\ p_{22} = P(0|-1) = F_n(1 + \theta) - F_n(1 - \theta) \\ p_{32} = P(-1|-1) = F_n(1 - \theta) \end{cases} \quad (45)$$

**Theorem 5.1.1:** The (2,3) DMC becomes BSC/SE when the pdf of the additive noise is an even function.

*Proof:* Given that the pdf is an even function, one can easily verify that  $F(-x) = 1 - F(x)$ .

Then according with (44) and (45) the following relation stands

$$p_{11} = p_{32}, \quad p_{21} = p_{22}, \quad p_{31} = p_{12} \quad (46)$$

Since  $F_N(\theta)$  is a strictly continuous and increasing function  $1 - \theta > -1 - \theta$ , we obtain that  $F_N(1 - \theta) > F_N(-1 - \theta)$  which corresponds to

$$p_{11} > p_{12} \quad (47)$$

Equations (46) and (47) are the relation constraints of the BSC/SE.

At this point, we have extended the results of [16] by showing that the (2,3) physical communication channel presented in Figure 21, is a BSC/SE channel in the presence of any noise that has an even probability distribution function. This further motivates our work to study the capacity SR behavior of this channel which was not presented in [19].

Using (44) and (45), we can re-write the (2,3) DMC matrix as:

$$\begin{aligned} M &= \begin{pmatrix} p_{11} & p_{21} & p_{31} \\ p_{12} & p_{22} & p_{32} \end{pmatrix} \\ &= \begin{pmatrix} 1 - F_N(-1 + \theta) & F_N(-1 + \theta) - F_N(-1 - \theta) & F_N(-1 - \theta) \\ 1 - F_N(1 + \theta) & F_N(1 + \theta) - F_N(1 - \theta) & F_N(1 - \theta) \end{pmatrix} \end{aligned} \quad (48)$$

By using (25) the capacity of the BSC/SE channel could then be rewritten below in (49) and it is plotted in Figure 25 for Gaussian, Laplace and Cauchy noise and a threshold  $\theta = 2$ .

$$\begin{aligned} C(X, Y) &= F_N(1 - \theta) \log_2 \left( \frac{F_N(1 - \theta)}{0.5(F_N(1 - \theta) - F_N(-1 - \theta)) + F_N(-1 - \theta)} \right) + \\ &F_N(-1 - \theta) \log_2 \left( \frac{F_N(-1 - \theta)}{0.5(F_N(-1 - \theta) - F_N(1 - \theta)) + F_N(1 - \theta)} \right) \end{aligned} \quad (49)$$

So far, we have shown that the (2,3) DMC in presence of some type of noise exhibit stochastic resonance. The range value for the threshold and the noise power in order for the (2,3) DMC to exhibit stochastic resonance and maximize the channel capacity is of interest.

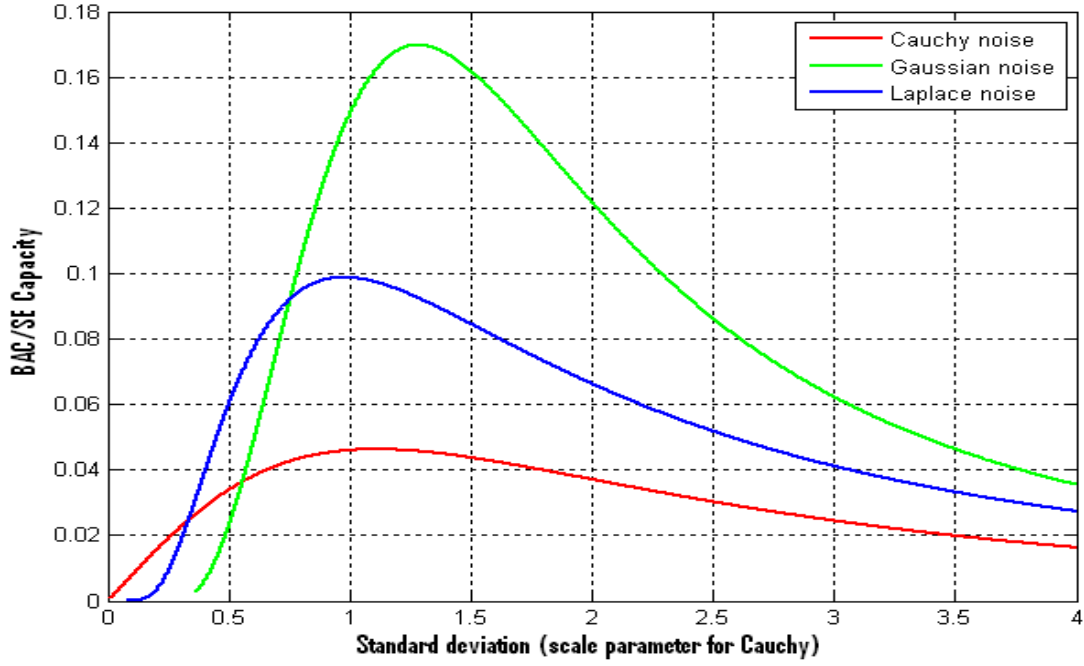


Figure 25. BAC/SE Capacity  $C$  of a threshold system ( $\theta = 2$ ) with three kinds of noise.

In the next section, in order find the range over which the (2,3) DMC exhibit SR, we will focus on the additive Gaussian noise, Pinsker and Helgert capacity bounds.

## 5.2 Stochastic Resonance and additive Gaussian noise

We start by re-plotting (49) in Figure 26 as a function of the threshold  $\theta$  and the variance  $\sigma$  (noise power). Since  $C(X, Y)$  is a function of  $\theta$  and  $\sigma$ , we will re-write it as follow,

$$C(X, Y) = C_{\theta}(\sigma) \quad (50)$$

We observe the phenomenon of SR on capacity over a specific range of  $\theta$  and noise power  $\sigma$ . In Figure 27, we plot the capacity of the BSC/SE for different values of the threshold  $\theta$ . To be more specific, in Figures 26 and 27, the SR appears only for  $\theta > 1$ . For the noise power  $\sigma \in [5, 10]$  and the threshold level  $\theta > 3$ , the capacity is vanishing to zero. Similar results were reported in [4], [5], and [9] for the (2,2) DMC. While these results are in concordance with the intuition that increasing the noise power on the channel will decrease the

capacity, the opposite, when the noise power decreases the capacity is also decreasing as it will be detailed in the next section.

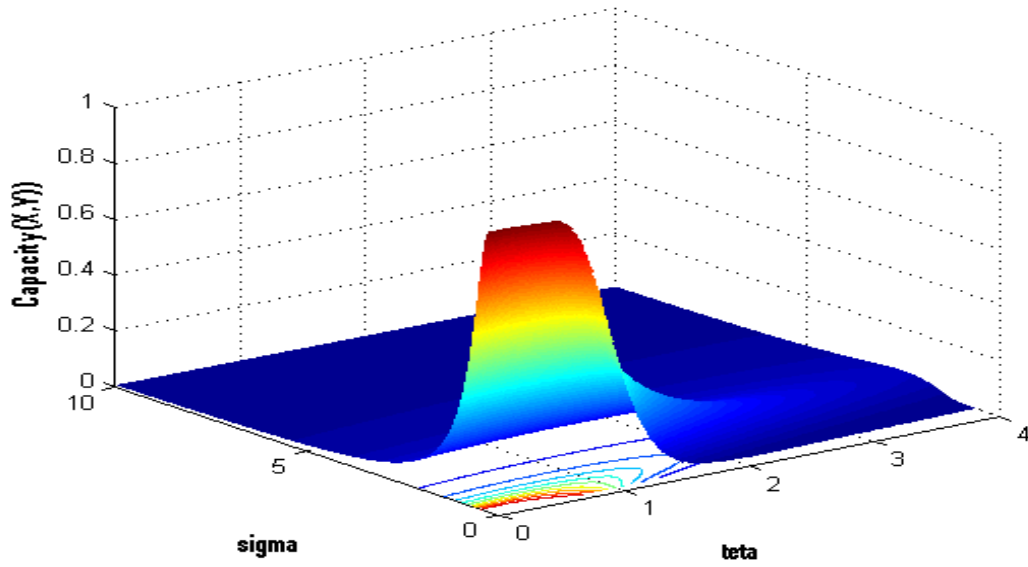


Figure 26. Capacity of BAC/SE as a function of  $\theta$  and  $\sigma$

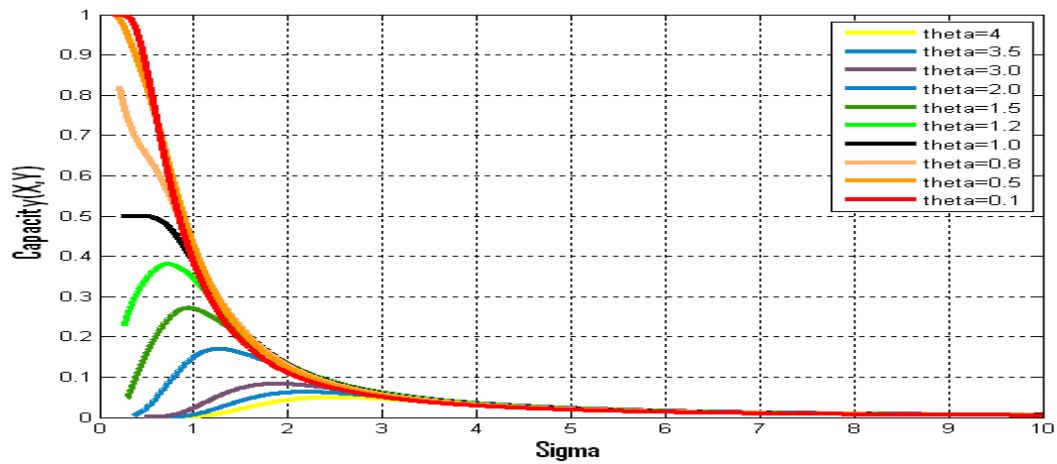


Figure 27. Capacity of BSC/SE for  $\theta = \{0.5, 0.6, 1, 1.5, 2, 2.5, 3, 3.5, 4\}$

### 5.2.1 Stochastic Resonance and Forbidden Interval Theorem in the case of the BSC/SE

In [20], the Forbidden Interval Theorems (FIT) in stochastic resonance are introduced. The FIT gives the necessary and the sufficient condition for stochastic resonance to occur. In general, the forbidden interval is the region or interval in which there is no stochastic resonance. A similar approach is reported in [21], where the Algebraic Information Theory (AIT) was used for the (2, 2) DMC to determine the forbidden interval. Given the close relation between partial ordering and the AIT, we will follow the steps of [21] to confirm our previous observation for the forbidden interval in the case of the BSC/SE.

**Definition 5.2.1** [21] A threshold system exhibits stochastic resonance (as a function of  $\sigma$ ) if and only if there exists  $0 < \sigma_1$  and  $0 < \sigma_2$  such that  $\sigma_1 < \sigma_2$  and  $C_\theta(\sigma_1) < C_\theta(\sigma_2)$

**Theorem 5.2.1:** The BSC/SE exhibits stochastic resonance if and only if the threshold  $\theta \notin [0, 1]$ .

*Proof:* We follow closely the proof used in [21] for the case of (2, 2) DMC. We will write the cdf of the Gaussian distribution with zero mean ( $F_n(\theta) = \frac{1}{\sigma\sqrt{2\pi}} \int_{-\infty}^{\theta} e^{-\frac{t^2}{2\sigma^2}} dt$ ) as the cdf of the standard normal cdf ( $\Phi(\theta) = \frac{1}{\sqrt{2\pi}} \int_{-\infty}^{\theta} e^{-\frac{t^2}{2}} dt$ ). By a change of variables we obtain  $F_n(\theta) = \Phi\left(\frac{\theta}{\sigma}\right)$

- For  $\theta \in [0, 1)$  as  $\sigma$  increases, since  $1 - \theta < 0$  we have  $a = \Phi\left(\frac{1-\theta}{\sigma}\right)$  decreases and  $b = 1 - \Phi\left(\frac{1+\theta}{\sigma}\right)$  increases. When  $a$  decreases and  $b$  increases, Theorem 4.2.1 tells us the capacity decreases. Therefore for  $\theta \in [0, 1)$ , as  $\sigma$  increases, the capacity decreases; therefore it does not exhibit stochastic resonance.
- For  $\theta = 1$ , as  $\sigma$  increases  $a = \Phi\left(\frac{1-\theta}{\sigma}\right) = 0.5$  and  $b = 1 - \Phi\left(\frac{2}{\sigma}\right)$  increases. When  $a$  is constant and  $b$  increases, Theorem 4.2.1 tells us the capacity decreases. Therefore for  $\theta = 1$ , as  $\sigma$  increases, the capacity decreases; therefore it does not exhibit stochastic resonance.

- For  $\theta > 1$ , as  $\sigma \rightarrow 0^+$ ,  $a \rightarrow 0$ ,  $b \rightarrow 0$  therefore  $C(a, b) \rightarrow 0$ . When  $\sigma \rightarrow \infty$ ,  $a \rightarrow \frac{1}{2}$ ,  $b \rightarrow \frac{1}{2}$  therefore  $C(a, b) \rightarrow 0$ . Since there exist  $\sigma > 0$  such that  $a \neq b$  meaning that  $C(a, b) \neq 0$ , we can conclude that the capacity increases for some interval of  $\sigma$ .

## 5.2 Stochastic Resonance and capacity bounds for (2, n) DMC

Due to the non-existence of a closed form expression for a (2, n) channel capacity in general and, the non-linear expression of the (2,3) channel capacity in particular, we will use the bounds (upper and lower) developed in [12] for the particular case of the (2,3) DMC in order to examine the phenomenon of stochastic resonance.

In [12],[13] it has been proven that any (2, n) DMC with 2 inputs and n outputs with the transition matrix  $M = \begin{pmatrix} p_{1,1} & \dots & p_{n-1,1} & p_{n,1} \\ p_{1,2} & \dots & p_{n-1,2} & p_{n,2} \end{pmatrix}$ , where  $p_{n,1} = 1 - p_{1,1} - \dots - p_{n-1,1}$  and  $p_{n,2} = 1 - p_{1,2} - \dots - p_{n-1,2}$ , can be approximated by: a lower bound called the Pinsker bound, that we denote by L, and upper bound, the Helgert bound, that we denote U. The Pinsker and Helgert bounds are defined as follows:

$$L \leq C \leq U$$

where

$$L = \frac{1}{8 \ln(2)} \left[ \left( \sum_{i=1}^{n-1} |p_{i,1} - p_{i,2}| \right) + |p_{n,1} - p_{n,2}| \right]^2$$

$$U = \max \left( \sum_{i=1}^{n-1} p_{i,1} ; \sum_{i=1}^{n-1} p_{i,2} \right) - \left( \sum_{i=1}^{n-1} \min(p_{i,1} ; p_{i,2}) \right)$$

For a (2,3) DMC, the above expressions are reduced to

$$\frac{1}{8 \ln(2)} [|p_{11} - p_{12}| + |p_{21} - p_{22}| + |p_{31} - p_{32}|]^2 \leq \max(p_{11} + p_{21}; p_{12} + p_{22}) - \min(p_{11}; p_{12}) - \min(p_{21}; p_{22}) \quad (51)$$

We have shown previously that using the threshold model given in Figure 21 and modeling noise as a standard Gaussian distribution we have the following equality:

$$p_{11} = p_{32}, p_{21} = p_{22}, p_{31} = p_{12}, p_{21} = p_{22}, p_{11} \geq p_{12}, \text{ and } p_{32} \geq p_{31}$$

Using these relations and (51) we have

$$\frac{1}{2 \ln(2)} (p_{11} - p_{12})^2 \leq C \leq p_{11} - p_{12} \quad (52)$$

Using (44) and (45) we have

$$\frac{1}{2 \ln(2)} (F_N(1 - \theta) - F_N(-1 - \theta))^2 \leq C \leq F_N(1 - \theta) - F_N(-1 - \theta) \quad (53)$$

Finally, we have

$$L = \frac{1}{2 \ln(2)} (F_N(1 - \theta) - F_N(-1 - \theta))^2 = f(\theta, \sigma) \quad (54)$$

$$U = F_N(1 - \theta) - F_N(-1 - \theta) = g(\theta, \sigma) \quad (55)$$

The Pinsker lower capacity bound  $L$  and the Helgert upper capacity bound  $U$  are plotted in Figure 28 and 29, respectively. In Figure 30, the lower and the upper capacity bounds along with the capacity of the BSC/SE are plotted for different values of the threshold  $\theta$ . We noted that, just as mentioned in [9], the bounds capture the increasing/decreasing behavior of the capacity and exhibit stochastic resonance for the threshold level  $\theta > 1$ .

Following similar work done in [21], we will use the bounds to find the optimum noise given a threshold that will maximize the channel capacity. The above lower and upper bounds are given by:

$$L = \frac{1}{2 \ln(2)} (F_N(1 - \theta) - F_N(-1 - \theta))^2 \text{ and } U = F_N(1 - \theta) - F_N(-1 - \theta).$$

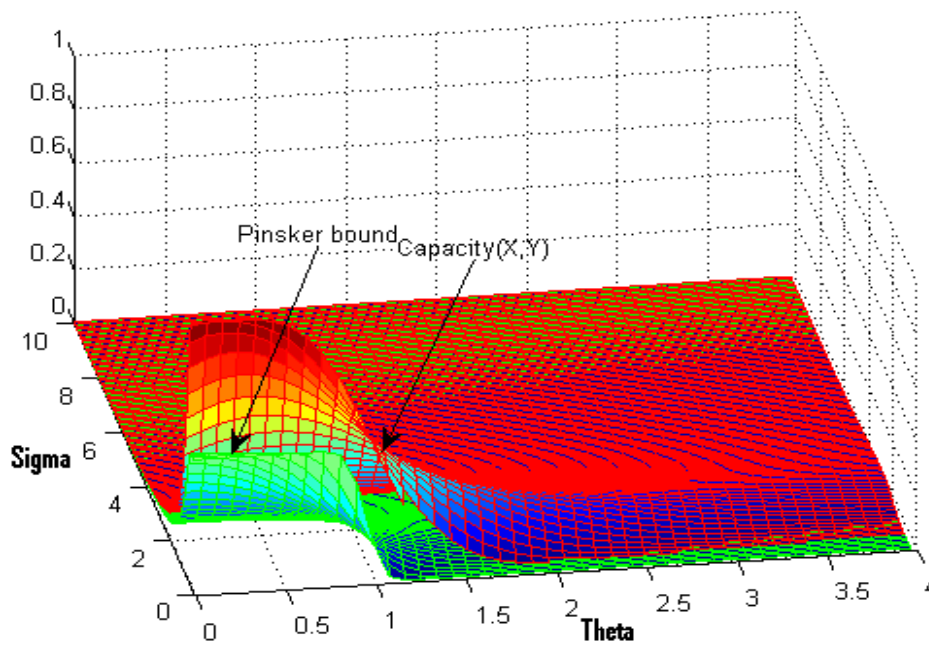


Figure 28. (2,3) DMC and Pinsker capacity Bound

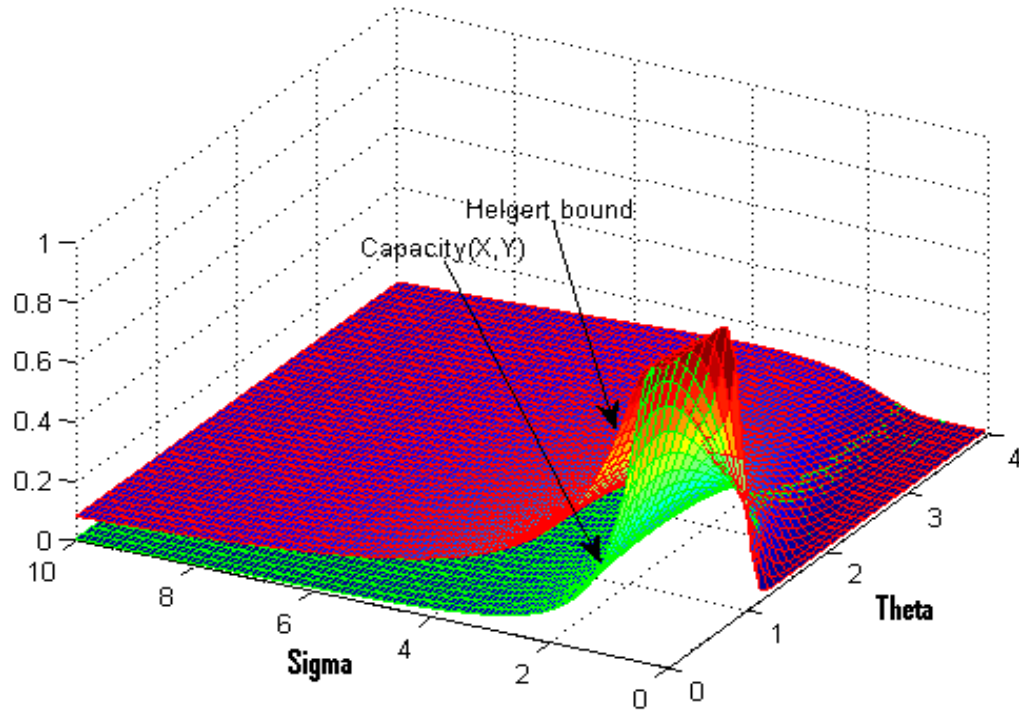


Figure 29. (2,3) DMC and Helgert capacity Bound

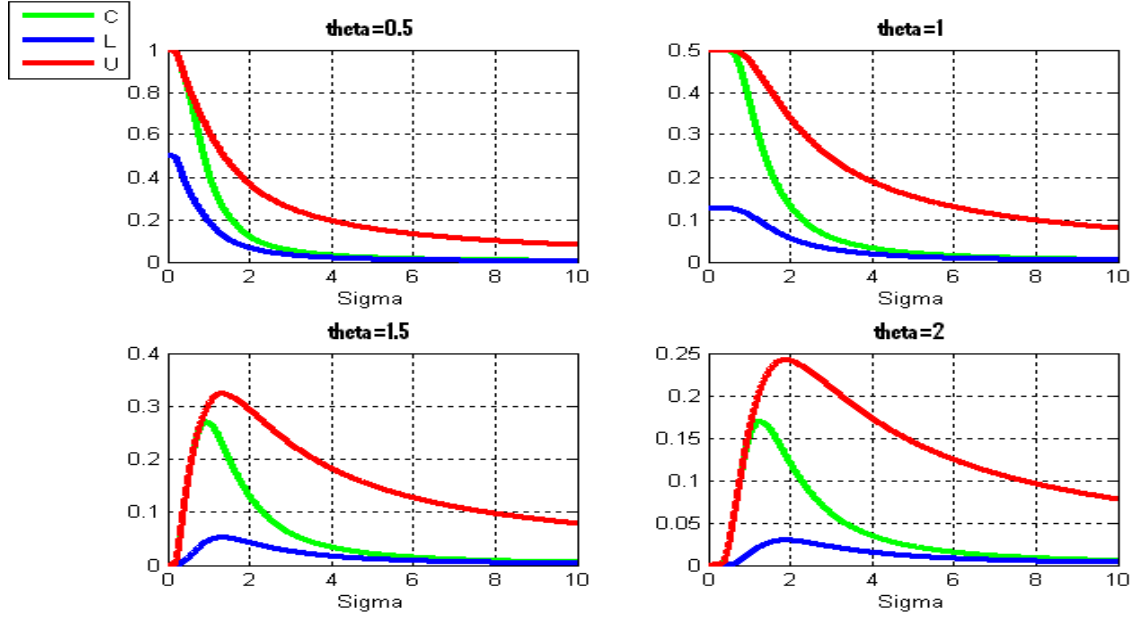


Figure 30. Capacity(C), Pinsker (L) and Helgert (U) bounds for different values of  $\theta$

### 5.3 Optimal values for threshold and noise levels

The optimal values of correlated noise and threshold level are of great interest. As in [21], our goal is to find the critical points of the capacity bounds. In order to find the critical points, we derive the partial derivatives  $\frac{d}{d\sigma}L(\theta, \sigma)$  and  $\frac{d}{d\sigma}U(\theta, \sigma)$  of the lower and upper bounds, and find the solution to the equations  $\frac{d}{d\sigma}L(\theta, \sigma) = 0$  and  $\frac{d}{d\sigma}U(\theta, \sigma) = 0$ , respectively.

The partial derivative of the bounds with respect to  $\sigma$  will have the same critical points because:

$$\begin{aligned} \frac{d}{d\sigma}L(\theta, \sigma) &= \frac{1}{\ln(2)} (F_N(1 - \theta) - F_N(-1 - \theta))' (F_N(1 - \theta) - F_N(-1 - \theta)) \\ &= \frac{1}{\ln(2)} \frac{d}{d\sigma}U(\theta, \sigma) (F_N(1 - \theta) - F_N(-1 - \theta)) \end{aligned}$$

Thus, solving

$$\frac{d}{d\sigma}L(\theta, \sigma) = 0$$

is equivalent to

$$\frac{d}{d\sigma}U(\theta, \sigma) = 0$$

which implies that they both have the same critical points. Therefore, we only focus

$$\text{on } \frac{d}{d\sigma} U(\theta, \sigma) = F_N(1 - \theta) - F_N(-1 - \theta).$$

We have

$$\begin{aligned} \frac{d}{d\sigma} U(\theta, \sigma) &= \frac{d}{d\sigma} (F_N(1 - \theta) - F_N(-1 - \theta)) = \\ &= \frac{d}{d\sigma} \frac{1}{\sigma\sqrt{2\pi}} \int_{-1-\theta}^{1-\theta} e^{-\frac{t^2}{2\sigma^2}} dt = \frac{-1}{\sigma^2\sqrt{2\pi}} \left[ (1 - \theta) e^{-\frac{(1-\sigma)^2}{2\sigma^2}} - (-1 - \theta) e^{-\frac{(-1-\sigma)^2}{2\sigma^2}} \right] \end{aligned}$$

Solving for  $\sigma$ ,  $\frac{d}{d\sigma} U(\theta, \sigma) = 0$ , we obtain

$$\ln\left(\frac{-1 + \theta}{1 + \theta}\right) = \frac{-4\theta}{2\sigma^2}$$

For  $\theta > 1$  and  $\sigma > 0$ , we finally have:

$$\sigma = \sqrt{\frac{2\theta}{\ln\left(\frac{1+\theta}{-1+\theta}\right)}} \quad (57)$$

The above relation gives us the optimum power noise  $\sigma$  as a function of  $\theta$ . In Figure 31, we plot (57),  $\sigma = f(\theta)$ , in blue and its inverse,  $f^{-1}(\theta)$ , in red. The plots depicted in Figure 31 provide theoretically two opportunities to improve the channel capacity, either by adding or reducing noise depending on the threshold or by simply adjusting the threshold depending on the noise level. It is important to mention that from the plot of Figure 31, we see that as  $\theta$  increases,  $\sigma \rightarrow \theta$ . That is because  $\lim_{\theta \rightarrow \infty} \sigma - \theta = 0$ , which means that  $\theta = \sigma$  is an oblique asymptote to  $\sigma = f(\theta)$  and  $\theta = f^{-1}(\sigma)$

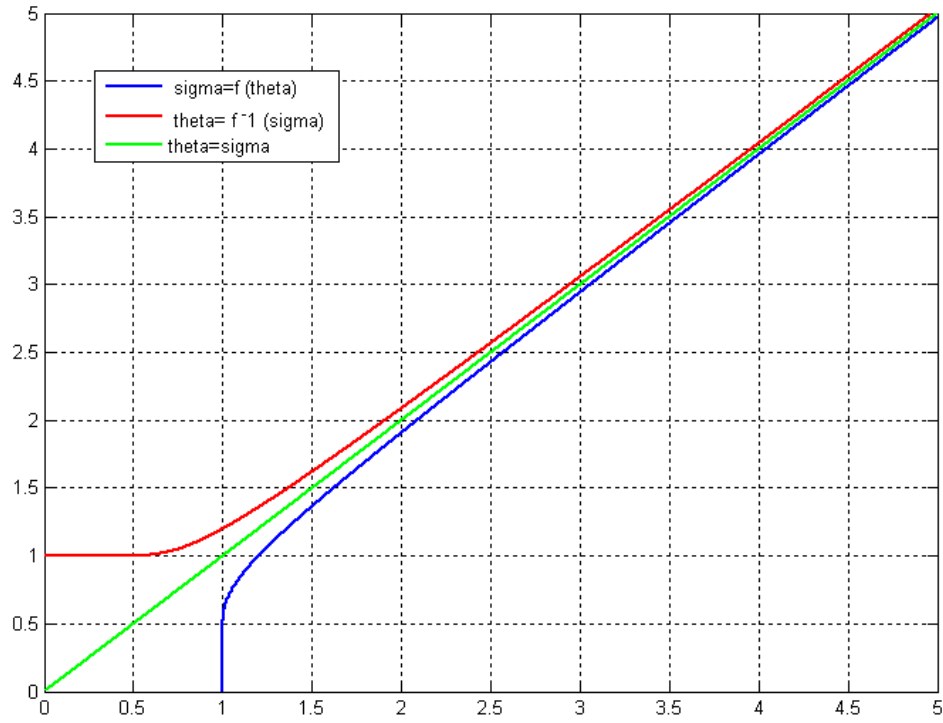


**Figure 31. Optimal noise power and threshold for stochastic resonance, with a scalable factor**

In this chapter, we have evaluated the SR phenomenon in the BSC/SE in presence of additive Gaussian, Laplace and Cauchy noise. In the particular case of the Gaussian noise, the forbidden interval is determined. Due to the non-linearity and the complexity of the analytical expression of the channel capacity, we use Pinsker lower and Helgert upper capacity bounds to also evaluate SR in BSC/SE, for which the optimal noise power in function of the threshold value is obtained.

## Chapter 6 Conclusions and future work

In this thesis, we have introduced a partial ordering for the BSC/SE which is a particular case of the BAC/SE and (2,3) DMC. We analyzed the general (2,3) DMC and established the relations between the BAC/SE, BSC/SE, BSC and the BEC. We demonstrated that in presence of the noise with even probability distribution function the general (2,3) DMC becomes the BSC/SE. Our partial ordering is based on channel convexity, majorization theory and directional derivative. We are able to give a partial ordering for the BSC/SE under specific conditional probability between channel input and channel outputs constraints.

In addition, we studied the threshold based stochastic resonance behavior of binary-input ternary-output DMC. The physical communication channel model is used to analyze the channel capacity behavior of the BSC/SE in the context of the stochastic resonance phenomenon. In presence of Gaussian noise, Laplace noise and Cauchy noise, the BSC/SE exhibit SR. For the particular case of the Gaussian noise, the results of the partial ordering are used to identify the forbidden interval. Due to the complexity and the non-linearity of the general (2, n) DMC capacity, the Pinsker lower and Helgert upper capacity bounds are used to analyze SR for the (2,3) DMC. Similar to the BSC/SE capacity, the capacity bounds exhibit SR. Based on these bounds, we analytically derived the optimum noise power level depending on the threshold level that will maximize the (2,3) DMC capacity.

The results of this thesis clearly indicate how one could compare channel capacity under the condition that applied without using the analytical relation of the capacity or the capacity bounds. They also demonstrate how one could improve the capacity of the binary threshold communication channel by changing the noise power or the threshold level.

In this thesis, the focus was on the Gaussian noise, Laplace noise and Cauchy noise, all with zero mean  $\mu = 0$  ( $x_0 = 0$  for Cauchy noise). In future research we will extend these results to noise distribution with different mean values (different location parameters). In addition we will use more practical underwater noise models to study the SR phenomenon in the (2,3) DMC.

## REFERENCES

- [1] C.E Shannon and W.W Weaver, "The Mathematical Theory of Communication," *University of Illinois press*, Urbana, IL, 1949.
- [2] Thomas M. Cover and Joy A. Thomas," Elements of Information Theory," *Second Edition, John Wiley and Sons*, 2006.
- [3] Paul Cotaé "Blind Doppler Estimation and Compensation in the Underwater Communications" *Technical report submitted to the Naval Research Laboratories*, Washington DC, Sept 2009.
- [4] François Chapeau-Blondeau," Noise Enhanced Capacity via Stochastic Resonance in an Asymmetric Binary Channel," *Physical Review E*, 55(2):2016-2019, 1997.
- [5] François Chapeau-Blondeau, "Periodic and Aperiodic Stochastic Resonance with Output Signal-to-noise Ratio Exceeding that at the Input," *International Journal of Bifurcation and Chaos*, vol.9, No1:267-272, 1999.
- [6] K. Chatzikokolaskis and K. Martin ,"A monotonicity principle for information theory",*Electronic Notes in Theoretical computer science* 218(2008)111-129.
- [7] Paul Cotaé and Ira S. Moskowitz," On the Partial Ordering of the Discrete Memoryless Channels Arising in Cooperative Sensor Networks," *4th IFIP International Conference on New Technologies, Mobility and Security, NTMS 2011*, pp.1-6, Paris, France, February 2011.
- [8] H.J. Helgert, "A Partial Ordering of Discrete Memoryless Channels", *IEEE Transactions on Information Theory* , vol. IT-3,no.3, pp.360-365,July 1967.
- [9] Ira S. Moskowitz, Paul Cotaé, Pedro N. Safier, and Daniel L. Kang," Capacity Bounds and Stochastic Resonance for Binary Input Binary Output Channels," *Proc. of the IEEE Computing, Communications & Applications conference, ComComAP 2012*, Hong Kong,pp.61-66,Jan. 2012.
- [10]François Chapeau-Blondeau, "Stochastic Resonance and the Benefit of Noise in Nonlinear Systems," *Noise, Oscillators and Algebraic Randomness – From Noise in Communication Systems to Number Theory. pp. 137-155*; M. Planat, ed., *Lecture Notes in Physics, Vol. 550*, Springer (Berlin) 2000.
- [11]Paul Cotaé, Ira S. Moskowitz and Myong H. Kang, "Eigenvalue Characterization of the Capacity of Discrete Memoryless Channels with Invertible Channel Matrices," *Proceedings IEEE 44th Annual Conference on Information Sciences and Systems-CISS 2010*, Princeton University,pp.1-6, March 2010.
- [12]Ira S. Moskowitz," Approximations for the Capacity of Binary Input Discrete Memoryless Channels," *In Proceedings 44<sup>th</sup> Annual Conf. on Information Science and Systems, CISS 2010*,Princeton ,NJ,USA, March 2010.
- [13]Ira S. Moskowitz," An Approximation of the Capacity of a Simple Channel," *43<sup>rd</sup> Annual Conf. on Information Science and Systems, CISS 2009*,Baltimore ,MD,USA, June 2009.
- [14]Paul Cotaé and T.C. Yang "A cyclostationary blind Doppler estimation method for underwater acoustic communications using direct-sequence spread spectrum signals," *8<sup>th</sup> International conf. on Communications, COMM 2010*, Bucharest, July 2010.
- [15]Ira S. Moskowitz and Paul Cotaé," Channel Capacity Behavior for Simple Models of Optical Fiber Communication," *8<sup>th</sup> International conf. on Communications, COMM 2010*, Bucharest, pp.1-6, July 2010.
- [16]Roland Kamdem, Paul Cotaé and Ira S. Moskowitz, "Threshold Based Stochastic Resonance for the Binary-Input Ternary-Output Discrete Memoryless Channel," *accepted at 7<sup>th</sup> IASTED International Conf. on Communication, Internet and Information Technology, CIIT 2012*,Baltimore, May 2012.
- [17]François Chapeau-Blondeau," Stochastic Resonance and the Benefit of Noise in Nonlinear Systems," *Noise, Oscillators and Algebraic Randomness – From Noise in Communication Systems to Number Theory. pp. 137-155*; M. Planat, ed., *Lecture Notes in Physics, Vol. 550*, Springer (Berlin) 2000.
- [18]Sanya Mitaim, Bart Kosko,"Adaptive Stochastic Resonance in Noisy Neurons Based on Mutual Information ," *IEEE Trans on Neural Networks Vol.15,No.6*, Nov 2004.

- [19] Mark Damian McDonnell, "Theoretical Aspects of Stochastic Signal Quantization and Suprathreshold Stochastic Resonance," *PhD thesis, The University of Adelaide*, Australia, Feb.2006.
- [20] Bart Kosko, Sanya Mitiam, Ashok Patel and Mark M. Wilde, "Applications of Forbidden Interval Theorem in Stochastic Resonance, " In *Applications of Nonlinear Dynamics ,Understanding Complex Systems*, pages 71-89.Springer-Verlag, 2009.
- [21] Ira S. Moskowitz, Paul Cota, Pedro N. Safier,"Algebraic Information Theory and Stochastic Resonance for Binary-Input Binary-Output Channels ," *Proceedings IEEE 46th Annual Conference on Information Sciences and Systems-CISS 2012*, Princeton University, March 17-19, pp.1-6, March 2012.
- [22] Paul Cota, et. all "Design and Application of a Distributed and Scalable Underwater Wireless Sensor Acoustic Networks" *2009 Annual ASEE Global Colloquium on Engineering Education*, Budapest, Hungary, Oct. 12-15, 2009.
- [23] R. A. Silverman,"On Binary Channels and their Cascades," *IRE Trans. Information Theory*, Vol.1,no.,pp.19-27,Dec 1995.
- [24] C.E. Shannon, "A note on a partial ordering for communication channels, "*Information and control*,Vol.1, pp.390-397,1958.
- [25] H.J. Helgert, "A Partial Ordering of Discrete Memoryless Channel," *IEEE Transactions on Information Theory*, vol.1, no.3, pp.360-365, July 1967.
- [26] A.W. Marshall and I. Olkin, *Inequalities: Theory of Majorization and its applications* .New York: Academic, 1979.
- [27] Patrick M. Fitzpatrick "Advanced Calculus," *American Mathematical Society*, 2009.

## Appendix

### Derivation of the Channel Capacity of the Binary Asymmetry Channel with Symmetry Erasure

In this section, we use the Kuhn-Tucker conditions to derive the analytical solution for the capacity achieving input probability distribution for Binary Asymmetric Channel with Symmetric Erasure (BAC/SE).

We recall from Chapter 2 that the channel capacity of the (2,3) DMC is characterized by a binary input random variable  $X = \{x_1, x_2\}$ , a ternary output random variable  $Y = \{y_1, y_2, y_3\}$  and a  $(2 \times 3)$  channel transition probability matrix  $M$  defined by  $M = \begin{pmatrix} p_{11} & p_{21} & p_{31} \\ p_{12} & p_{22} & p_{32} \end{pmatrix}$ . The entries of this matrix are the  $p_{ij} = p(y_j|x_i)$  which represent the probability of receiving the symbol  $y_j$  given that the symbol  $x_i$  was sent. We have shown in (15) that the capacity of the (2,3) DMC is defined by

$$C = \max_x \sum_{i=1}^2 \sum_{j=1}^3 p(x_i) p(y_j|x_i) \log_2 \frac{p(y_j|x_i)}{\sum_{k=1}^2 p(x_k) p(y_j|x_k)} \quad (\text{A.1})$$

where  $p(x_1) = 1 - p(x_2) = x$

The BAC/SE is a particular case of the (2,3) DMC with  $p_{21} = p_{22}$

*Theorem A.1:* [15] An input distribution given by  $\{p(x_1), p(x_2)\}$  achieves capacity if and only if there exists a constant  $C$  such that

$$\sum_{j=1}^3 p_{j,i} \log_2 \frac{p_{j,i}}{\sum_{k=1}^2 p(x_k) p_{j,k}} = C, \forall i \text{ with } p(x_i) > 0 \quad (\text{A.2})$$

$$\sum_{j=1}^3 p_{j,i} \log_2 \frac{p_{j,i}}{\sum_{k=1}^2 p(x_k) p_{j,k}} \leq C, \forall i \text{ with } p(x_i) = 0 \quad (\text{A.3})$$

For  $i = 1$ , we can rewrite (A.2) as follow

$$C = p_{11} \log_2 \frac{p_{11}}{p(x_1)p_{11} + p(x_2)p_{12}} + p_{21} \log_2 \frac{p_{21}}{p(x_1)p_{21} + p(x_2)p_{22}}$$

$$+p_{31}\log_2 \frac{p_{31}}{p(x_1)p_{31}+p(x_2)p_{32}} \quad (\text{A.4})$$

For  $i = 2$ , (A.2) becomes

$$\begin{aligned} C = p_{12}\log_2 \frac{p_{12}}{p(x_1)p_{11} + p(x_2)p_{12}} + p_{22}\log_2 \frac{p_{22}}{p(x_1)p_{21} + p(x_2)p_{22}} \\ + p_{32}\log_2 \frac{p_{32}}{p(x_1)p_{31}+p(x_2)p_{32}} \end{aligned} \quad (\text{A.5})$$

Since  $p_{21} = p_{22}$ , by equaling (A.4) to (A.5), we obtain

$$\begin{aligned} \frac{p_{11}^{p_{11}}p_{31}^{p_{31}}}{[x(p_{11} - p_{12}) + p_{12}]^{p_{11}}[x(p_{31} - p_{32}) + p_{32}]^{p_{31}}} \\ = \frac{p_{12}^{p_{12}}p_{32}^{p_{32}}}{[x(p_{11}-p_{12})+p_{12}]^{p_{12}}[x(p_{31}-p_{32})+p_{32}]^{p_{32}}} \end{aligned} \quad (\text{A.6})$$

For simplicity, we define

$$m = x(p_{11} - p_{12}) + p_{12}, n = x(p_{31} - p_{32}) + p_{32} \text{ and } t = \frac{p_{12}^{p_{12}}p_{32}^{p_{32}}}{p_{11}^{p_{11}}p_{31}^{p_{31}}}$$

Replacing  $m, n$  and  $t$  in (A.6), we obtain

$$m^{p_{12}-p_{11}}n^{p_{32}-p_{31}} = t \quad (\text{A.7})$$

Given that  $M$  is a stochastic matrix, we have,

$$p_{11} + p_{21} + p_{31} = p_{12} + p_{22} + p_{32} = 1 \quad (\text{A.8})$$

Since  $p_{21} = p_{22}$ , from (A.8), we have

$$p_{12} - p_{11} = p_{32} - p_{31}, \quad (\text{A.9})$$

Combining (A.9) and (A.7), we finally obtain

$$\frac{n}{m} = t^{\frac{1}{p_{11}-p_{12}}} \quad (\text{A.10})$$

Replacing  $m, n$  and  $t$  by their relations in (A.10), we obtain,

$$\frac{x(p_{31}-p_{32})+p_{32}}{x(p_{11}-p_{12})+p_{12}} = \left( \frac{p_{12}^{p_{12}} p_{32}^{p_{32}}}{p_{11}^{p_{11}} p_{31}^{p_{31}}} \right)^{\frac{1}{p_{11}-p_{12}}} \quad (\text{A.11})$$

Solving (A.11) for  $x$ , we obtain

$$x = \frac{p_{12}-p_{32} \left( \frac{p_{11}^{p_{11}} p_{31}^{p_{31}}}{p_{12}^{p_{12}} p_{32}^{p_{32}}} \right)^{\frac{1}{p_{11}-p_{12}}}}{(p_{12}-p_{11})-(p_{32}-p_{31}) \left( \frac{p_{11}^{p_{11}} p_{31}^{p_{31}}}{p_{12}^{p_{12}} p_{32}^{p_{32}}} \right)^{\frac{1}{p_{11}-p_{12}}}} \quad (\text{A.12})$$

The relation (A.12) represents the input probability distribution that achieves the capacity. With  $x$  found, one obtain the analytical solution of the BAC/SE by replacing (A.12) in to (A.1).